NATIONAL ADVISORY COMMITTEE FOR AERONAUTICS

TECHNICAL MEMORANDUM

No. 1189

THEORETICAL ANALYSIS OF STATIONARY POTENTIAL FLOWS AND BOUNDARY LAYERS AT HIGH SPEED

By K. Oswatitsch and K. Wieghardt

TRANSLATION

"Theoretische Untersuchungen über stationäre Potentialströmungen und Grenzschichten bei hohen Geschwindigkeiten"

Lilienthal-Gesellschaft für Luftfahrtforschung Bericht S 13/1.Teil, pp. 7-24

Washington

April 1948

NATIONAL ADVISORY COMMITTEE FOR AERONAUTICS

TECHNICAL MEMORANDUM NO. 1189

THEORETICAL ANALYSIS OF STATIONARY POTENTIAL FLOWS AND BOUNDARY LAYERS AT HIGH SPEED*

By K. Oswatitsch and K. Wieghardt

The present report consists of two parts. The first part deals with the two-dimensional stationary flow in the presence of local supersonic zones. A numerical method of integration of the equation of gas dynamics is developed. Proceeding from solutions at great distance from the body the flow pattern is calculated step by step. Accordingly the related body form is obtained at the end of the calculation.

The second part treats the relationship between the displacement thickness of laminar and turbulent boundary layers and the pressure distribution at high speeds. The stability of the boundary layer is investigated, resulting in basic differences in the behavior of subsonic and supersonic flows. Lastly, the decisive importance of the boundary layer for the pressure distribution, particularly for thin profiles, is demonstrated.

P A R T I

NOTATION

p	pressure
ρ	density
T	absolute temperature
κ	ratio of specific heats
$n = \frac{2}{\kappa - 1}$	

*"Theoretische Untersuchungen über stationäre Potentialströmungen und Grenzschichten bei hohen Geschwindigkeiten." Lilienthal-Gesellschaft für Luftfahrtforschung Bericht S 13/1.Teil, pp. 7-24.

μ	coefficient of friction
$\underline{w}$	velocity vector
w	magnitude of velocity
u, v	velocity components
Φ	velocity potential
c	velocity of sound
c^*	critical velocity of sound
$Ma = w/c$	Mach number
$F = 1 - Ma^2$	
$\theta = \rho/\rho_\infty$	stream density
Re^*	Reynolds number of the displacement thickness
δ	boundary-layer thickness
δ^*	displacement thickness
ϑ	momentum thickness
f	stream filament section
r	radius of curvature of the stream line
N	normal to the stream line
H	maximum bump elevation
R	related radius of curvature

Subscript ∞ refers to the conditions in the free-stream region, subscript α to the outer flow, subscript w to the wall. Subscript m refers to the chamber or drum values in the phase quantities and in the velocity to the highest obtainable value. The quantities of state in part I are made dimensionless by the chamber quantities and the velocities by the highest velocity obtainable.

PART I

1. NOTES ON THE CHARACTERISTICS OF COMPRESSIBLE POTENTIAL FLOWS

The equation of gas dynamics is derived by means of the energy equation rather than the adiabatic equation as customary. A simple formula is obtained for the stream density which is valid in a wide range about the critical velocity of sound. By applying this formula a simplified equation of gas dynamics is derived which in the transition zone from subsonic to supersonic, for small velocity components v, describes the processes very accurately. Lastly, the problem of flow around a cylindrical body, symmetrical in two directions, is analyzed. It is found that, from a certain flow velocity on, located above the critical velocity, no maximum velocity can occur at the point of maximum body thickness.

In the description of a gas flow the most general case involves six unknown functions, namely, the three components of the velocity and the three phase quantities of the gas, the pressure p, the density ρ, and the absolute temperature T. The equation of state of the gas permits the temperature to be expressed in terms of the pressure and density, thus leaving five unknown functions for the calculation of which the three Euler equations and the continuity equation are available. For the missing equation it is customary to use the adiabatic curve to eliminate the pressure and density from the equation and so arrive at an equation between the velocity components, that is, the so-called equation of gas dynamics. However, it appears to be unknown that for the derivation of the equation of gas dynamics the assumption of the adiabatic is not necessary at all, but that the use of the energy theorem itself is sufficient. This derivation is briefly carried out in the following, while having recourse to the vector method.

Pressure, density, and temperature are made nondimensional by the corresponding "chamber quantities" p_m, ρ_m, T_m; that is, the quantities of state at velocity 0, and all occurring velocities and velocity components by the maximum obtainable velocity, that is, the velocity at pressure 0. With $\underline{w}$ denoting the velocity vector, c_p the specific heat at constant pressure, and κ the ratio of the specific heats this maximum velocity is

$$w_m^2 = 2c_p T_m = 2\frac{\kappa}{\kappa - 1}\frac{p_m}{\rho_m}$$

The equation of energy of an ideal gas in stationary flow has expressed nondimensionally - the following simple form

$$w^2 + \frac{p}{\rho} = 1 \tag{1.1}$$

and the corresponding continuity condition reads

$$\operatorname{div} \underline{w} + \frac{w}{\rho} \operatorname{grad} \rho = 0 \tag{1.2}$$

The oft repeated quantity

$$n = \frac{2}{\varkappa - 1}$$

has a physical significance; it indicates the degrees of freedom of a molecule. For air $n = 5$ is very exact.

The Euler equation is then written as

$$\left(\operatorname{grad} \frac{w^2}{2} - \underline{w} \times \operatorname{rot} \underline{w}\right) \varkappa n = - \frac{1}{\rho} \operatorname{grad} p \tag{1.3}$$

The quantity xn enters the equation through the nondimensional notation.

Pressure and density are eliminated by forming the gradient of the energy equation, thus obtaining

$$0 = \operatorname{grad} \underline{w}^2 + \frac{1}{\rho} \operatorname{grad} p + (\underline{w}^2 - 1) \frac{1}{\rho} \operatorname{grad} \rho$$

Scalar multiplication by $\underline{w}$ and application of (1.2) and (1.3) gives the equation of gas dynamics

$$(1 - \underline{w}^2) \operatorname{div} \underline{w} + n\underline{w} \operatorname{grad} \frac{w^2}{2} = 0 \tag{1.4}$$

This equation is written here in a form where the velocity of sound is already eliminated and only the flow velocity itself is present. We will use this equation in the next section.

For an insight into the potential flow properties in the speed range of Ma = 1 the just derived equation is much too complicated. So the processes in a flow filament are analyzed, unsteady variations

and friction processes excluded so that adiabatic changes of state can be assumed. The energy equation (1.1) then affords a connection between velocity and density, and the stream density $w\rho$ can be represented as a function of the velocity w:

$$\theta(w) = \rho w = w(1 - w^2)^{n/2} \tag{1.5}$$

It is known that this function reaches a maximum at the point where the velocity is exactly equal to the velocity of sound. This particular point is generally denoted as the critical speed of sound c^*. With f as the section of a flow filament the continuity equation reads $f\theta = \text{const}$. The speed c^* is therefore characterized by the fact that a flow filament for this value of w reaches a smallest possible cross section. For $w > c^*$ as for $w < c^*$ the flow filament section is greater.

Less familiar is the smallness of the stream density changes over a very substantial speed range. To indicate it $\frac{\theta}{\theta^*}$ is represented for $x = 1.40$ in the range of $0.5c^* < w < 1.5c^*$ in figure 1. Quantity θ^* denotes the value of θ for $w = c^*$, the same applies to the derivatives of θ. This characteristic of the stream density is of decisive significance for the effect of the boundary layer on the flow, as will be shown elsewhere.

Consider the function θ in the vicinity of the maximum developed and signify its derivative with θ^*_w, θ^*_{ww}, etc. Now it is found that the parabola

$$\frac{\theta}{\theta^*} = 1 + \frac{1}{2} c^{*2} \frac{\theta^*_{ww}}{\theta^*} \left(\frac{w}{c^*} - 1\right)^2 \tag{1.6}$$

is already sufficiently accurate for a wide speed range. This approximation is indicated by dashes in figure 1. The calculation for the coefficient of the quadratic term gives the simple result

$$\frac{1}{2} c^{*2} \frac{\theta^*_{ww}}{\theta^*} = -\frac{\kappa + 1}{2} = -\frac{n + 1}{n} \tag{1.6}$$

The equation (1.6) serves in good stead for the derivation of a simplified dynamic gas equation for two-dimensional flows on the limiting assumptions that the y component of velocity w, signified by v, is small compared to the velocity of sound and that u, the x component of the velocity, does not differ too much from the velocity of sound. The stream density $w\rho$ can be

replaced by $u\rho = \theta(u)$ and the equation of continuity (1.2) on applying the same omissions as effected with respect to the terms with the factor v for the derivation of the Prandtl law, can be written as

$$\frac{1}{\rho}\frac{\partial}{\partial x}(u\rho) + \frac{\partial v}{\partial y} = \frac{u}{\theta}\theta_u \frac{\partial u}{\partial x} + \frac{\partial v}{\partial y} = 0$$

The coefficient of $\frac{\partial u}{\partial x}$ depends only on u; it is simply a different method of expressing the well-known quantity $1 - Ma^2$. Assuming, aside from the smallness of v, that $\frac{u}{\theta}\theta_u$ can be regarded as constant results in the Prandtl-Glauert analogy. If this coefficient were plotted against u in the vicinity of the sonic velocity, it would show that it can assume negative as well as positive values and at $u = c^*$ is equal to zero. So the premise of constancy of this quantity can no longer be maintained, especially since the derivative θ_u changes signs at sonic velocity, as seen from figure 1. The variations of $\frac{u}{\theta}$ on the other hand are no more weighty than the variations of the entire coefficient anywhere in the range of not too high subsonic speeds. Thus in support of Prandtl's law $\frac{u}{\theta}$ can very well be put equal to this quantity in the free-stream region, but not for θ_u. This equantity is computed by (1.6) and gives

$$-\frac{u_o}{\theta_o} - \frac{\theta^*}{c^*}(\kappa + 1)\left(\frac{u}{c^*} - 1\right)\frac{\partial}{\partial x}\left(\frac{u}{c^*} - 1\right) + \frac{\partial}{\partial y}\frac{v}{c^*} = 0$$

The subscript o denotes the quantities in the free-stream region. Using the notation

$$U \equiv \frac{u_o}{c^*}\frac{\theta^*}{\theta_o}(\kappa + 1)\left(\frac{u}{c^*} - 1\right); \quad V = \frac{u_o}{c^*}\frac{\theta^*}{\theta_o}\frac{v}{c^*}(\kappa + 1) \tag{1.7}$$

gives for $\frac{v}{c^*} \ll 1$ and $\frac{u}{c^*} \approx 1$ the simplified equation of gas dynamics

$$-U\frac{\partial U}{\partial x} + \frac{\partial V}{\partial y} = 0 \tag{1.7}$$

U can be positive and negative. Here also the introduction of a velocity potential is accompanied, although in simplified form, by the undersirable change of the equation from the elliptical to the hyperbolic type. To secure solutions which have supersonic zones by an analytical method it is advisable to find solutions of (1.7), because it combines the simplifying assumption of small v

with a very accurate description of the processes in the critical sonic speed range. This was the reason for the brief derivation of the equation.

The fact that the flow filament section has a minimum at the critical speed may, under certain circumstances, have very characteristic consequences for the velocity distribution at the appearance of supersonic zones on bodies, as will be demonstrated for the case of two-dimensional flow past a body that is symmetrical about two mutually perpendicular axes. The flow direction is to be along one body axis, that is, the angle of attack equal to zero.

The flow is to be adiabatic and irrotational, the latter characteristic being expressed by

$$\frac{\partial w}{\partial N} = -\frac{w}{r} \tag{1.8}$$

where N is the normal to the streamline and r its radius of curvature. The sign for N is so chosen that it is positive when the normal points out from the radius of curvature. Equation (1.8) holds exactly for all two-dimensional potential flows. By the continuity condition in the form,

$$\theta f = \text{Constant}$$

and the freedom from rotation (1.8) the flow is completely defined. The origin of the coordinate system x and y is placed in the center of the body, axis x is made coincident with the flow direction (fig. 2), and the area of positive y value analyzed. The cylindrical body is visualized as being exposed to a flow velocity which leads to the formation of a supersonic zone near the thickest part of the body and it is assumed that in every stream filament the maximum velocity is reached at the point $x = 0$, an assumption which certainly should be fulfilled for subsonic flows. A point on the y—axis with supersonic speed must have a maximum stream filament width, a point with subsonic speed, a minimum of stream filament width. In the supersonic region the curvature of the streamlines on the positive portion of the y— axis must decrease less rapidly than on concentric circles, in the subsonic zone the stream line curvature must decrease more rapidly than for concentric circles. Hence no great error is introduced when in the vicinity of the point on the y— axis where sonic velocity is reached, the streamlines are replaced by concentric circles, and it will not lead us far astray when this is assumed up to a value of y equal to twice the distance from the cylinder of the point with the critical sonic

velocity c^*. After the streamline curvatures are approximately known the velocity distribution on the $y-$axis in this zone is completely defined by (1.8). If the piece which the body cuts off from the $y-$axis is denoted by H and the radius of curvature of the profile on the $y-$axis by R, its velocity distribution is

$$\frac{u}{u_{y=H}} = \frac{R}{R - H + y} \tag{1.9}$$

According to (1.6) it may be stated that the volume of flow through a section of the $y-$axis is then greater than on an identical section of the free stream, if at a particular point the inequality

$$u_o < u < 2c^* - u_o$$

is fulfilled. Since the velocity distribution for $x = 0$ is defined by (1.9) up to the constant $u_{y=H}$, it also is the difference in through flow volume for $y > H$ in the free-stream region and on the $y-$axis. It may now be asked at what value of the constants the absolute amount of this through flow difference reaches its highest possible value and the answer is found in the fairly accurate equation

$$u_{y=H} = 2c^* - u_o \tag{1.9a}$$

that is, that the stream density on the $y-$axis must nowhere be less than in the free stream. For a simple picture it is imagined that (1.9) with the constant (1.9a) is applicable up to the attainment of speed u_o and that from this y value on, the constant flow velocity prevails. This break may occur at the value $y = y_o$ for which the equation reads

$$u = u_o \text{ for } \frac{y_o - H}{R} = 2\left(\frac{c^*}{u_o} - 1\right)$$

As near the body more can flow by than on a strip of equal width in the free-stream region, because of the increase in density, we must proceed from the cylinder only as far as the free stream is displaced. The result is therefore a highest possible value of H, denoted by H_{max}, which is given by the equation

$$\vartheta_o H_{max} = \int_{y=H_{max}}^{y=y_o} (\vartheta - \vartheta_o)\, dy \tag{1.10}$$

The integrand is given by (1.6), (1.9), (1.9a), H is to be replaced by H_{max}, since u is equal to w on the y—axis. The evaluation of (1.10) gives the following relation between flow velocity and $\frac{H_{max}}{R}$.

TABLE I

$\frac{u_o}{c^*}$	0.70	0.75	0.80	0.85	0.90	0.95	1.00
$\frac{H_{max}}{R}$	0.053	0.026	0.013	0.0059	0.0020	0.0004	0.

The extension of the speed by pieces at $y = y_o$ unquestionably introduces an error; but it can only cause a shift in H_{max}, while not changing the existence of such a value. In the subsonic zone a streamline may be regarded as a bump and the residual rise in through flow volume due to increase in velocity computed by an approximation process that applies in the subsonic range. The result then is a finite variation of the integral in (1.10) and a correspondingly different H_{max}. The possibility of a speed increase in y direction in the subsonic region must be rejected, as it would invalidate the present considerations. Hence it is seen that the assumption cannot be applied to all bodies and therefore the following principle:

To each flow velocity u_o, there corresponds a definite ratio H_{max}/R. If the ratio H/R exceeds this limit for a body symmetrical in two mutually perpendicular directions and lying along the flow direction, there is no flow for which velocity maximums can be reached on the entire y—axis.

It must be expected that the maximum speeds on the y—axis disappear only in the supersonic range. But since it cannot be assumed that velocity maximums in the supersonic range disappear on a part of the y—axis while a velocity maximum appears on the body, we are led to the following principle.

From a definite value of H/R on, for bodies and flow directions of the described type, there is no flow at which a speed maximum with local supersonic zone is reached at the point of maximum thickness of the body.

A boundary point for these specific values of H/R is given in table I.

In the subsonic zone this principle has no analogy.

2. METHOD FOR THE NUMERICAL INTEGRATION OF THE EQUATION OF GAS DYNAMICS

A numerical - graphical method is indicated for finding solutions of the equation of gas dynamics with supersonic zones, by progressive calculation of the entire flow, starting from an exact solution at great distances from the body. The exact body form follows at the end from the shape of the streamlines. Exceeding the sonic velocity causes no special difficulties or peculairities.

Limited to two-dimensional, irrotational flows with $\underline{w} = \operatorname{grad} \Phi$ past a cylindrical body, equation (1.4) gives for the velocity potential φ a nonlinear differential equation of the second order

$$D[\Phi] = \left[1 - (n+1)\left(\frac{\partial\Phi}{\partial x}\right)^2 - \left(\frac{\partial\Phi}{\partial y}\right)^2\right]\frac{\partial^2\Phi}{\partial x^2} + \left[1 - \left(\frac{\partial\Phi}{\partial x}\right)^2 - (n+1)\left(\frac{\partial\Phi}{\partial y}\right)^2\right]\frac{\partial^2\Phi}{\partial y^2} \qquad (2.1)$$

$$- 2n\,\frac{\partial\Phi}{\partial x}\,\frac{\partial\Phi}{\partial y}\,\frac{\partial^2\Phi}{\partial x\,\partial y} = 0; \quad n = \frac{2}{\kappa - 1}$$

The zero point of the coordinate system is placed in the body, its dimensions are of the order of magnitude of unity, and the flow strikes the body along the positive x-axis. The boundary conditions for Φ then read:
$\frac{\partial\Phi}{\partial N} = 0$ at the body itself, N denoting the normal, and at infinity for $z \equiv \sqrt{x^2 + y^2} \to \infty$ $\frac{\partial\Phi}{\partial y} \to 0$ and $\frac{\partial\Phi}{\partial x} \to u_o$ = (dimensionless) flow velocity.

On passing through the local velocity of sound $\left(\sqrt{\frac{1}{n+1}}\right)$, equation (2.1) changes from the elliptic to the hyperbolical type. For this case the exact integration has been successfully secured for single specific examples only. For the subsonic range several general approximate solutions are available, the simplest and best known of which is the solution Φ_2 obtained by the Prandtl rule. This satisfies equation (2.1) better as the body becomes more slender and the distance from the body becomes greater.

The following method is therefore indicated. Compute the Prandtl solution Φ_p for the entire flow and attempt to secure the correction φ in such a way that $\Phi_p + \varphi = \Phi$ becomes a solution of the complete equation (2.1). As the analytical calculation of φ is too complicated, a numerical method is advisable, starting from the outside $(z \gg 1)$ where $\varphi \approx 0$, and progressively continuing inwardly toward the body. The exact body shape follows at the end of the calculation from the streamline distribution; however it is to be suspected that it essentially remains similar to the form of the Prandtl solution.

For this purpose the differential equation for $\varphi = \Phi - \Phi_p$ is set up; Φ_p is an exact solution of the considerably simplified equation (2.1):

$$(1 - Ma_o^2)\frac{\partial^2 \Phi_p}{\partial x^2} + \frac{\partial^2 \Phi_p}{\partial y^2} = 0$$

with

$$Ma_o = \frac{u_o}{c_o} = \sqrt{n \frac{u_o^2}{1 - u_o^2}} \tag{2.2}$$

The subscript o refers to the conditions at infinity, φ_p fulfills the complete equation (2.1) up to an error ϵ_p which can be computed by means of (2.2):

$$D\left[\Phi_p\right] \equiv \epsilon_p = -\left\{(Ma_o^2 + n)\left(\frac{\partial \Phi_p}{\partial x}\right)^2 + \left[(n+1)\,Ma_o^2 - n\right]\left(\frac{\partial \Phi_p}{\partial y}\right)^2 - Ma_o^2\right\}\frac{\partial^2 \Phi_p}{\partial x^2} - 2n\,\frac{\partial \Phi_p}{\partial x}\,\frac{\partial \Phi_p}{\partial y}\,\frac{\partial^2 \Phi_p}{\partial x\,\partial y} \tag{2.3}$$

Putting $\Phi = \Phi_p + \varphi$ in (2.1) and regarding it as a differential equation for φ, ϵ_p follows as term of zero degree in φ. As $\varphi \ll \Phi_p$ in the entire range, it is assumed that it applies to the derivatives as well. Merely the terms of the zero and first degree

and the greatest term of the second degree in φ need to be included. There results

$$\left[1-\left(\frac{\partial\Phi_p}{\partial x}\right)^2-(n+1)\left(\frac{\partial\Phi_p}{\partial y}\right)^2\right]\frac{\partial^2\varphi}{\partial y^2}$$

$$=-\epsilon p-\left[1-(n+1)\left(\frac{\partial\Phi_p}{\partial x}\right)^2-\left(\frac{\partial\Phi_p}{\partial y}\right)^2\right]\frac{\partial^2\varphi}{\partial x^2}$$

$$+2\left[\left(Ma_o^2+n\right)\frac{\partial^2\Phi_p}{\partial x^2}\frac{\partial\Phi_p}{\partial x}+n\frac{\partial^2\Phi_p}{\partial x\,\partial y}\frac{\partial\Phi_p}{\partial y}\right]\frac{\partial\varphi}{\partial x}$$

$$+2\left\{\left[(n+1)Ma_o^2-n\right]\frac{\partial^2\Phi_p}{\partial x^2}\frac{\partial\Phi_p}{\partial y}+n\frac{\partial^2\Phi_p}{\partial x\,\partial y}\frac{\partial\Phi_p}{\partial x}\right\}\frac{\partial\varphi}{\partial y}$$

$$+2n\frac{\partial\Phi_p}{\partial x}\frac{\partial\Phi_p}{\partial y}\frac{\partial^2\varphi}{\partial x\,\partial y}+2(n+1)\frac{\partial\Phi_p}{\partial x}\frac{\partial^2\varphi}{\partial x^2}\frac{\partial\varphi}{\partial x} \qquad (2.4)$$

The better Φ_p satisfies the equation of gas dynamics, the easier is the determination of φ. So, at great distances from the body the equation can be substantially simplified. For $z \gg 1$, especially on slender bodies, $\frac{\partial\Phi_p}{\partial y} \ll \frac{\partial\Phi_p}{\partial x}$; hence we can put $\frac{\partial\Phi_p}{\partial y}=0$ and $\frac{\partial\varphi}{\partial y}=0$ in 2.4 but in contrast to the Prandtl rule consider the variation of $\frac{\partial\Phi}{\partial x}$. Since $\varphi \to 0$ for $z \to \infty$, the term of the second degree is omitted also. And equation (2.4) is simplified to

$$\frac{\partial^2\varphi}{\partial y^2}=-\left(F-F_o+F'\frac{\partial\varphi}{\partial x}\right)\frac{\partial^2\Phi_p}{\partial x^2}-F\frac{\partial^2\varphi}{\partial x^2}; \qquad (2.5)$$

with

$$F\left(\frac{\partial\Phi_p}{\partial x}\right)\equiv 1-Ma^2=\frac{1-(n+1)\left(\frac{\partial\Phi_p}{\partial x}\right)^2}{1-\left(\frac{\partial\Phi_p}{\partial x}\right)^2}$$

and

$$F' \cong \frac{dF}{d\left(\frac{\partial \Phi_p}{\partial x}\right)} = - \frac{2n\left(\frac{\partial \Phi_p}{\partial x}\right)}{\left[1\left(\frac{\partial \Phi_p}{\partial x}\right)^2\right]^2}$$

This equation could also be derived from (1.7); F is an abbreviation for $\frac{u}{\theta}\theta_u$.

The boundary condition for $z \to \infty$ is $\varphi = 0$ where the Prandtl rule applies exactly. On the other hand, however, the disturbance of the flow by the body is very extended when the flow velocity approaches sonic velocity. It is therefore necessary to determine an initial approximation for φ analytically so as not to be compelled to start at unduly great distances. For this purpose (2.5) is transformed further. While $Ma = Ma_o$, by the Prandtl rule, hence $F = F_o$, the more exact term $F = F_o + F' \cdot \left(\frac{\partial \Phi_p}{\partial x} - u_o\right)$, so that

$$F_o \frac{\partial^2 \varphi}{\partial x^2} + \frac{\partial^2 \varphi}{\partial y^2} = - F' \left[\left(\frac{\partial^2 \Phi_p}{\partial x^2} + \frac{\partial^2 \varphi}{\partial x^2}\right)\left(\frac{\partial \Phi_p}{\partial x} - u_o\right) + \frac{\partial^2 \Phi_p}{\partial x^2}\frac{\partial \varphi}{\partial x}\right] \qquad (2.7)$$

There $\frac{\partial^2 \varphi}{\partial x^2}$ can be ignored with respect to $\frac{\partial^2 \Phi_p}{\partial x^2}$, and it is assumed that $\frac{\partial \varphi}{\partial x} \ll \frac{\partial \Phi_p}{\partial x} - u_o$ at great distances; for example, in the calculated case: For a parallel flow and dipole, $\frac{\partial \Phi_p}{\partial x} - u_o$ dies down as $1/z^2$, but $\frac{\partial \varphi}{\partial x}$ as $1/z^4$. Hence finally:

$$F_o \frac{\partial^2 \varphi}{\partial x^2} + \frac{\partial^2 \varphi}{\partial y^2} = (F_o - F) \frac{\partial^2 \Phi_p}{\partial x^2} \qquad (2.10)$$

All the equations for the process are now available. The general process of calculation is as follows: First determine the entire field of flow of the incompressible fluid numerically, and then the compressible approximate solution by the Prandtl rule for a fixed Ma number of the flow velocity. The correction φ on a strip for great y follows from (2.10). From here on φ is computed numerically, step by step. At great distance from the body we

therefore first use equation (2.5) and later in the neighborhood of the body the more complete equation (2.4). Having thus determined φ for the entire field, the stream lines and therefore the body contour itself, as well as pressure and velocity distribution, are obtained from $\Phi = \Phi_p + \varphi$. Naturally the process can be built on another approximate solution; however, the formulas probably become simplest when the Prandtl rule is used.

For the present the range of application of this method is confined to the flows where the Prandtl rule affords a good approximate solution and the fundamental assumption $\varphi << \Phi_p$ is actually fulfilled.

Excluded are accordingly flows around not sufficiently slender bodies, as well as areas in which the velocity of sound is substantially exceeded. This also manifested itself in the calculated example. Flow around a cylinder (circular in the incompressible case) at Ma = 0.7454. The calculation was perfectly smooth into the supersonic range, where it had to be broken off especially since $\frac{\partial \varphi}{\partial x}$ and $\frac{\partial^2 \varphi}{\partial x \, \partial y}$ quickly rose to the order of magnitude of $\frac{\partial \Phi_p}{\partial x}$ and $\frac{\partial^2 \Phi_p}{\partial x \, \partial y}$ but exceeding the sonic velocity itself involved no difficulties.

In principle we can also free ourselves from the approximation that $\varphi \ll \Phi_p$, when in the formulation of equation 2.4 we consider terms of the third degree in φ; the length of the calculation, however, becomes disproportionately large. In another more appropriate method the assumption $\varphi \ll \Phi_p$ is omitted and the tedious calculation of Φ_p in the entire field of flow is eliminated. The previously described φ method is utilized only for computing the initial values for large Σ. The new method is as follows: Φ_p is evaluated at large distances from the body for $y \gg y_1$; where y_1 is chosen so large that the error of the Prandtl solution is sufficiently small; φ is evaluated from equation 2.10. This affords the exact solution of the dynamic gas equation $\Phi = \Phi_p + \varphi$ in an initial strip. From here on Φ itself is calculated step by step. The width of the initial strip from $-x_1$ to $+ x_2$[1] must extend upstream and downstream from the body so that for all y at $x \leq - x_1$ and $x \geq x_2$ the Prandtl rule is applicable with sufficient accuracy. From y_1 on, where Φ is then known, $\frac{\partial^2 \Phi}{\partial y^2}$ is graphically extrapolated to $y_1 - \frac{1}{2} \Delta y$ for certain

---

[1]For bodies which are symmetrical relative to the y-axis also, x_1 is naturally $= x_2$.

fixed abscissae x (Δy is the length of the step; it can be assumed quite large at first, and reduced again later in proximity of the body). Next

$$\left.\frac{\partial\Phi}{\partial y}\right|_{y_1-\Delta_y} = \left.\frac{\partial\Phi}{\partial y}\right|_{y_1} - \left.\frac{\partial^2\Phi}{\partial y^2}\right|_{y_1-\frac{1}{2}\Delta y} \Delta y$$

is plotted against x and graphically differentiated, which gives $\left.\frac{\partial^2\Phi}{\partial y\,\partial x}\right|_{y_1-\Delta y}$. Plotting $\frac{\partial^2\Phi}{\partial y\,\partial x}$ against y and integrating gives

$$\left.\frac{\partial\Phi}{\partial x}\right|_{y_1-\Delta y} = \left.\frac{\partial\Phi}{\partial x}\right|_{y_1} + \int_{y_1}^{y_1-\Delta y} \frac{\partial^2\Phi}{\partial y\,\partial x}dy$$

Lastly the variation of $\left.\frac{\partial\Phi}{\partial x}\right|_{y_1}$ over x yields $\frac{\partial^2\Phi}{\partial x^2}$ by graphical differentiation. With it

$$\frac{\partial\Phi}{\partial x},\ \frac{\partial\Phi}{\partial y},\ \frac{\partial^2\Phi}{\partial y\,\partial x},\ \text{and}\ \frac{\partial^2\Phi}{\partial x^2}$$

are known for $y = y_1 - \Delta y$.

From the equation of gas dynamics (9.1), in which the simplification $\frac{\partial\Phi}{\partial y} = 0$ can be made so long as it is valid that $\frac{\partial\Phi}{\partial y} \ll \frac{\partial\Phi}{\partial x}$, $\frac{\partial^2\Phi}{\partial y^2}$ is calculated for the required x values and plotted against y. Then the calculation is repeated, $\frac{\partial^2\Phi}{\partial y^2}$ extrapolated for $y_1 - \frac{3}{2}\Delta y$ and so forth.

If the values of $\frac{\partial^2\Phi}{\partial y^2}$ computed for $y \geq y_1$, the value extrapolated at $y_1 - \frac{1}{2}\Delta y$ and that computed for $y_1 - \Delta y$ do not form a smooth curve, the step must be repeated with a differently extrapolated value for the particular abscissae. In this event it is better to reduce the length of the step. Since the differentiation

of the curves $\left.\frac{\partial\Phi}{\partial x}\right|_{y=\text{const.}}$ and $\left.\frac{\partial\Phi}{\partial y}\right|_{y=\text{const.}}$ is uncertain at the boundary points $x = -x_1$ and $x = x_2$, it is advisable to compute $\Phi = \Phi_p + \varphi$ also in two vertical strips $x \leq -x_1$ and $x \geq x_2$ and to join the progressively defined points to these edge strips.

The direction of integration for this step method must be chosen at right angles to the flow for the following reason. At flow around a body exposed to a flow along x. $\frac{\partial\Phi}{\partial x}$ is sure to be greater than $\frac{\partial\Phi}{\partial y}$ almost everywhere, especially in the supersonic zone. Thus at entry in a supersonic zone the coefficient of $\frac{\partial^2\Phi}{\partial x^2}$ in (2.1) goes through zero. This does not interfere in the above method since (2.1) is used for computing $\frac{\partial^2\Phi}{\partial y^2}$.

If, however, we integrate in the x-direction and solve equation (2.1) for $\frac{\partial^2\Phi}{\partial x^2}$, then difficulties will result. The coefficient of $\frac{\partial^2\Phi}{\partial y^2}$ can, on the other hand, disappear only far above the speed of sound where $\frac{\partial\Phi}{\partial y}$ is not important at the point under consideration. We can also prove this state of affairs with the help of characteristics. When discontinuities in the velocity or their derivatives appear we cannot integrate across a characteristic. On the other hand the characteristics of our flow become nearly vertical so that again we can not calculate in the x direction in this supersonic region.

3. ILLUSTRATIVE EXAMPLE

A flow symmetrical in x and y is computed for a Mach number of flow of 0.7454. The flows on smooth bumps with supersonic zones are obtained exactly, but on the other hand the flow past a closed body is obtained only with errors in the region of the stagnation point.

The described method is tried out on a very simple example; we start from the incompressible flow (subscript i) past a circular cylinder

$$\Phi_i = x_i + \frac{x_i}{x_i^2 + y_i^2} \tag{3.1}$$

the free-stream velocity and the radius are taken as unity. Prandtl's rule is applied to a fixed Mach number of flow Ma_o to which the dimensionless flow velocity

$$u_o = \left.\frac{\partial \Phi_p}{\partial x}\right|_{z \to \pm\infty} = \sqrt{\frac{Ma_o^2}{Ma_o^2 + n}}$$

corresponds. The abscissas for this transformation are contracted by $\sqrt{1 - Ma_o^2}$.

$$x \equiv x_p = \sqrt{1 - Ma_o^2}\, x_i \tag{3.2}$$

The ordinates remain the same: $y \equiv y_p = y_i$; so that

$$\frac{\partial \Phi_p}{\partial x} = u_o \frac{\partial \Phi_i}{\partial x_i} \text{ and } \frac{\partial^2 \Phi_p}{\partial x^2} = \frac{u_o}{\sqrt{1 - Ma_o^2}} \frac{\partial^2 \Phi_i}{\partial x_i^2} \tag{3.3}$$

To compute φ by equation (2.10) the coordinates x_i and $y = y_i$ are used, so that

$$\left(1 - Ma_o^2\right) \frac{\partial^2 \varphi}{\partial x^2} + \frac{\partial^2 \varphi}{\partial y^2} = \frac{\partial^2 \varphi}{\partial x_i^2} + \frac{\partial^2 \varphi}{\partial y^2}$$

$$= \frac{u_o}{\sqrt{1 - Ma_o^2}} \frac{\partial^2 \Phi_i}{\partial x_i^2} \left[\frac{1 - (n+1)\, u_o^2 \left(\partial \Phi_i / \partial x_i\right)^2}{1 - u_o^2 \left(\frac{\partial \Phi_i}{\partial x_i}\right)^2} - 1 + Ma_o^2 \right] \tag{3.4}$$

Development of the right-hand side for large $z_i \equiv \sqrt{x_i^2 + y^2}$ by using equation (3.1) gives for the first approximation, when

$$\xi = \frac{x_i^2}{z_i^2} \text{ and } \eta = \frac{y^2}{z_i^2} = 1 - \xi$$

$$\Delta\varphi(x_1, y) = -\frac{4Ma_o^4}{nu_o\sqrt{1 - Ma_o^2}}\frac{x_1}{z_1^6}(1 - 6\eta + 8\eta^2)$$

$$= -\frac{12Ma_o^4}{nu_o\sqrt{1 - Ma_o^2}}\frac{x_1}{z_1^6}\left(1 - \frac{10}{3}\xi + \frac{8}{3}\xi^2\right) \qquad (3.5)$$

A particular integral of this Poisson equation is obtained with the help of the separation formula $\varphi = \frac{x_1}{z_1^4} f(\xi)$. Thus the general solution is written

$$\varphi = \frac{-12Ma_o^4}{nu_o\sqrt{1 - Ma_o^2}}\frac{x_1}{z_1^4}\left[c - \left(\frac{4}{3}c - \frac{1}{6}\right)\xi - \frac{1}{6}\xi^2\right] + \varphi_{pot} \qquad (3.6)$$

with $\Delta\varphi_{pot} = 0$ and c arbitrary.

As boundary condition for φ the sole requirement is that it shall be small compared to φ_p, that is, decrease more rapidly than $\frac{1}{z_1}$. But for the rest φ_{pot} and c can be chosen at random. The physical meaning of this ambiguity is as follows: Owing to the disregarded terms of higher order in the formulation of (3.5) only the effects of the first order of the body at great distances are taken into account. But these are the same for different body forms. So the calculation yields different section forms, depending upon the choice of c and φ_{pot}. The manner in which c and φ_{pot} affect the body form cannot be evaluated until several examples have been worked out. Up to now only one such example has been worked out, owing to lack of time.

The Mach number of flow $Ma_o = \sqrt{5/9} = 0.7454$ had been specifically chosen. The dimensionless velocity is then $u_o = \sqrt{1/10} = 0.3162$ and $x \equiv x_p = \frac{2}{3}x_1$.

In (3.6) only half $\varphi_{pot} \equiv 0$ and $c = 1/8$ were assumed for simplicity, thus eliminating the linear term in ξ

$$\varphi = -\frac{5\sqrt{10}}{36}\frac{x_1}{z_1^4}\left(1 - \frac{4}{5}\xi^2\right) \tag{3.7}$$

with this φ the velocities (and their derivatives) of the exact solution $\Phi = \Phi_p + \varphi$ for $y = 10$ and $0 \leq x < 6$, as well as to $x = 6$, $0 \leq y \leq 10$ were computed and Φ was determined for $y < 10$ and $x < 6$ by the described step-by-step method. In view of the symmetry of flow relative to x and y the calculation in one quadrant was sufficient. The step length Δy up to $y = 1.5$ was $\Delta y = 0.5$; from there on 0.2.

While the exceeding of the sonic velocity (first at $y = 1.35$) caused no difficulties, the calculation could not be carried out to the body because of another reason but had to be broken at $y = 0.6$. For at $x \approx 0.6$ the horizontal components of the velocity $\frac{\partial \Phi}{\partial x}$ changes so rapidly for smaller ordinates y that the graphical differentiations became too uncertain to compute the next step. As is seen from the contour of constant velocity (fig. 3) a steady but still very sudden rarefaction occurs and on a point symmetrically situated with reference to $x = 0$ a compression occurs. This phenomenon would of course not be plain at a lower flow velocity, but it is certainly characteristic of the flow in proximity of the stagnation point where the speed increases quickly from subsonic to supersonic. For this point of the flow field another method must therefore be developed.

So while unable to obtain the flow around a finite body with a stagnation point, the data obtained thus far are nevertheless very informative for subsonic flows with supersonic zones. The calculated streamlines and lines of constant velocity are shown in figure 3. Visualizing, the lowest streamline in figure 3 as rigid wall, we get the flow along a smooth bump with a supersonic zone near the highest point. Since this streamline is already very steep for $x \approx 0.65$, it can be assumed that the velocity distribution around the finite body (with symmetry axes $x = 0$ and $y = 0.5$) indicated in figure 5 is fairly accurately reproduced by the dotted line. Incidentally, it is noted that even Prandtl's rule yields considerable errors near the stagnation point.

Figure 4 shows several streamlines magnified five times in elevation, along with the respective velocity distributions. Notwithstanding the similarity of the individual peaks the velocities differ considerably at various places. The velocity — and with it the pressure distribution of thin bodies — is therefore at high flow velocities markedly dependent upon the exact shape of the body.

Noteworthy also is the steep velocity increase at a point where the streamlines themselves are still comparatively flat.

The contours of equal velocity in the supersonic region prove the principle set up in section 1 according to which the highest speeds under certain assumptions do not occur at the point of maximum thickness of the body. Even the equation (1.9) applied for the derivation of this principle is satisfactorily confirmed in figure 6, where the velocities on the y-axis are plotted along with the hyperbola (dotted) that touches the curve $w(x = 0)/c^*$ at $w/c^* = 1$. From the far-reaching agreement of the curves it follows that in the vicinity of $w = c^*$ the expression $u = w(x = 0) = \frac{a}{b + y}$ is a good approximation. With this example the accuracy of table I can be checked. In view of the flow velocity of $u_c/c^* = 0.7746$ $H_{max}/R = 0.019$ would have to be expected according to this table, but by the calculated example it is proved that from $H_{max}/R = 0.031$ on, the speed maximum is no longer situated at the greatest ordinate. Thus, it is seen that table I is a good representation of the order of magnitude of H_{max}/R. The difference is attributable to the fact that the hyperbola used for the approximation gives too low speeds in the subsonic range.

PART II

4. INTRODUCTORY NOTES ON BOUNDARY LAYERS AT HIGH SPEEDS

Studies of the behavior of supersonic flows in parallel channels disclose that in the supersonic zone, principal flow and boundary flow are in unstable equilibrium in certain circumstances. An effect of the boundary layer on the principal flow in the zone of the critical speed is to be expected for the reason that here small variations in stream density cause considerable changes in speed. This is particularly plain in the calculation of the flow through a Laval nozzle at high subsonic speed with observance of the boundary layer.

In order to gain an insight into the condition of the boundary-layer flow at high speeds, which we will study in the following, consider an example from the sphere of incompressible flows, where the conditions are better controlled. We consider the circulation-free, incompressible, and stationary flow around a circular cylinder at a high but still subcritical Reynolds number. Computing the pressure distribution at the body with the

aid of the potential theory on the assumption that the cylinder has no dead-air region behind it and then calculating on the basis of this the boundary-layer conditions, say, with the aid of a refined Pohlhausen method, we find a separation point in the zone of rising pressure. It is found that the omission of the dead-air region was wrong. The pressure distribution on the body must therefore be computed with due allowance for the dead-air region and then it can be hoped to attain a result corresponding to reality when the dead-air region is so assumed that the related pressure distribution yields separation exactly at the starting point of the free streamline. This example shows that potential flow and boundary-layer flow usually depend upon each other. In general, we can say that the potential flow determines the boundary-layer flow, also that the boundary-layer flow determines the potential flow. The former can be stated with great approximation in flow without pressure rise.

It is a known experimental fact that for large expansions a flow simply does not follow the boundaries of the region; but it should be remembered that for the development of a dead-air region not the expansion of the stream filament but the fact of a pressure rise is decisive, which only in subsonic flows goes hand in hand with an increase in stream filament section. In supersonic flow on the other hand a contraction of the stream filament results in a pressure rise. Thus visualizing a parallel channel with a flow of $Ma > 1$ a too strong growth in boundary layer caused by some disturbance is followed by a pressure rise, which in turn favors a stronger growth in boundary layer. In contrast to subsonic flow, an unstable equilibrium of boundary layer and principal flow is involved in this instance and a very considerable boundary layer growth must be reckoned with in certain circumstances. It may, in a straight channel result in a sudden strong pressure rise at the flat wall and so in the formation of a dead-air region (fig. 7(a)). (Compare reference 11.) If the pressure rise is so great that the flow becomes subsonic, the relation of main flow and boundary-layer flow is stable again, the dead-air space cannot remain in this part of the channel. If a small pressure rise is involved of, say, a weaker oblique compressibility shock, the principal flow experiences a directional change in the sense of a channel contraction. The dead-air space must increase wedge-like, but this holds only over a short distance, otherwise the flow would have to revert into the subsonic range. It is therefore to be assumed that at an oblique compressibility shock, as met with in figure 7(a), the turbulent intermingling imposes a limit on the growth of the dead-air space. These qualitative reflections lead to the conclusion that in the range $Ma > 1$ an unstable state of equilibrium must be reckoned with in certain circumstances between principal - and boundary-layer flow, which may promote the formation of dead-air regions even at a flat wall.

A disturbance of the unstable state of equilibrium of principal and boundary-layer flow in the supersonic range is favored by the fact that any minor disturbance in a supersonic flow is propagated undamped along Mach lines. Thus, a pressure rise in a supersonic tunnel can be dispersed by a small disturbance far upstream; on the other hand, the pressure rise sets in again some distance downstream as we can also infer from our example.

The unstable behavior of the boundary layer in the supersonic zone must disappear when the principal flow approaches sonic velocity. In the critical speed range $w = c^*$, which is of particular interest in flows past bodies with high speed, the fact stands out that this is the range of maximum flow density. But the procedure in computing the incompressible flow past an airfoil is such that the pressure distribution is obtained from the potential flow without consideration of the displacement effect of the boundary layer, and then the boundary layer is computed with the aid of this pressure distribution. This is not permissible however in the region of the velocity of sound, because a minor variation in stream density θ exerts a very substantial effect on the speed. This is readily apparent in figure 4, where peaks with comparatively minor form changes produce very unlike pressure distributions. This effect increases with increasing flow velocity.

The effect of the boundary layer on the flow in the vicinity of the velocity of sound is illustrated by a simple example, which, although it involves no flow problem, is nevertheless informative for the appraisal of the displacement effect of boundary layers at high speeds. The velocity distribution in the nozzle used by Stanton (reference 1) for his experiments was computed by application of the simple flow filament theory, once without boundary layer, and once on the assumption of a laminar boundary layer. The boundary-layer calculation is made with the help of a process which will be explained in the following section. The initial value of momentum and displacement thickness at $x = -0.20$ was estimated. The dimensions of the nozzle are so small that it can be assumed that no turbulent transition takes place. Stanton's test series C is illustrated in figure 7(b). The velocities were determined by measuring the static pressure on the axis of the axially symmetrical nozzle (lower test points) and adjacent to the wall (upper test points). The theoretical curves by Oswatitsch and Rothstein (reference 2) and the flow filament solution with and without boundary layer allowed for are included for comparison. The former was computed only as far as the separation point. It is seen that the asymmetry is reproduced qualitatively correct by the flow filament solution with boundary layer taken into account. The displacement thickness at the narrowest point of the nozzle is not quite 2 percent of the nozzle radius. Computing the velocity

distribution for the same nozzle in incompressible flow with and without consideration of the boundary layer, the results in both cases are essentially even lines. Even at speeds about 15 percent below those of test C, any boundary-layer effect is quite insignificant. This may be taken as proof that the asymmetry in nozzle flows which at the most, manifest local supersonic zones, are caused by boundary-layer effect. As to making the computation, only the following is mentioned. That one gets at first the distribution of the displacement thickness from the stream filament solution and then a new stream filament solution taking into account the calculated displacement thickness is proof in itself that such an iterative procedure is permissable at very high subsonic speeds. Displacement thickness and stream filament solution are obtained step-wise at the same time in the downstream direction.

The influence of the boundary layer on a submerged body will be handled in section 7. Our example, however, shows that we cannot hope to obtain results that correspond to the real process in some degree, for the flow problem with high velocity, without examining the boundary layer. We then have to remove, in practice or experiment, the influence of the boundary layer, perhaps by suction.

5. CALCULATION OF DISPLACEMENT THICKNESS OF LAMINAR AND TURBULENT COMPRESSIBLE BOUNDARY LAYERS

For more accurate calculations on boundary-layer effect in flows at high speed, formulas for the variation of the displacement thickness are necessary. This is done in this section, first for the laminar and then for the turbulent boundary layers. In the derivation of the formulas for laminar boundary layer a refined Pohlhausen method is given for computing laminar compressible boundary layers for given pressure distribution.

Inasmuch as the pressures in the compressible zone transverse to the flow direction in the boundary layer is also to be regarded as constant, the relative density variations within the boundary layer are in amount equal to the relative temperature variations. Thus, if sonic velocity prevails in the outer flow the relative density variation inside the boundary layer amounts to about 20 percent, since stagnation point temperature can be approximately assumed at the wall. So, at not too high supersonic speeds a qualitatively identical behavior in the boundary layer and in the incompressible range is to be expected.

So as not to exclude the possibility of compressibility shocks beforehand, the flow outside of the boundary layer is called outer- or-principal flow instead of potential flow.

Being primarily interested in the behavior of the displacement thickness, the behavior of other quantities is studied only to the extent that it appears in the result without loss of time. This is the case in the study of laminar boundary layers, where the momentum thickness is comparatively easily obtained and the displacement thickness derived from it.

The process is based upon an improved Pohlhausen method in conjunction with the reports by Bohlen (reference 3) and Walz (reference 4).

Boundary-layer equation and continuity condition for the stationary case are written as follows

$$\left.\begin{aligned} \rho u \frac{\partial u}{\partial x} + \rho v \frac{\partial u}{\partial y} &= -\frac{dp}{dx} + \frac{\partial}{\partial y}\left(\mu \frac{\partial u}{\partial y}\right) \\ \frac{\partial}{\partial x}(\rho u) + \frac{\partial}{\partial y}(\rho v) &= 0 \end{aligned}\right\} \qquad (5.1)$$

The coordinate system is chosen in the usual manner so that x is tangential and y normal to the contour of the body. Thus, in the general case, x, y imply no Cartesian coordinates in the following: μ is the friction coefficient dependent on temperature. The quantities p, ρ, u, and v are not made dimensionless. It further is assumed that the boundary-layer thickness is small relative to the radius of curvature of the wall, so that curvature effects can be disregarded. The second Navier-Stokes equation gives then exactly as for incompressible flow the result that p is merely dependent on x, but not on y, which in the boundary-layer equation was already evidenced by formation of the ordinary derivative of p.

After integration of the boundary-layer equation over y, the application of the continuity condition gives the von Kármán momentum equation which is written in the form

$$\frac{d}{dx}\left(\rho_a u_a^2 \vartheta\right) + \rho_a u_a \frac{du_a}{dx} \delta^* = \mu_w \left(\frac{\partial u}{\partial y}\right)_w \qquad (5.2)$$

The subscript w indicates the values at the wall, subscript a those in the outer flow. In the momentum equation displacement thickness and momentum thickness are defined by

$$\delta^* \equiv \int_0^\delta \left(1 - \frac{\rho u}{\rho_a u_a}\right) dy; \quad \vartheta \equiv \int_0^\delta \frac{\rho u}{\rho_a u_a}\left(1 - \frac{u}{u_a}\right) dy \tag{5.3}$$

where δ is the so-called boundary-layer thickness, which is now chosen so great that δ^* and ϑ can be regarded as independent of δ. The displacement thickness has the physical significance that the through flow volume in the boundary layer is reduced by an amount that, on the assumption of pure potential flow, is equivalent to a shift of the wall by piece δ^* in positive y direction.

Equation (5.2) can also be given the form

$$u_a \frac{d}{dx}\frac{\rho_a \vartheta^2}{\mu_w} + \frac{\rho_a \vartheta^2}{\mu_w}\frac{du_a}{dx}\left(2\frac{\delta^*}{\vartheta} + 4 - M_a^2\right) = 2\left(\frac{\partial}{\partial \frac{y}{\vartheta}}\frac{u}{u_a}\right) \tag{5.2a}$$

Aside from the usual assumptions with the aid of which the boundary-layer equations are derived, no restrictions of any kind have been made so far. Only the problem without heat transfer on the wall, the so-called thermometer problem, is treated in the following. Further we will make one approximation, by which we will specify the form of the boundary-layer profile by only one parameter in addition to the Mach number of the outside flow. Next it is necessary to make an assumption concerning the configuration of the density profile. Having seen that in the vicinity of the critical velocity the velocity profile especially might be decisive, while the density variation is unimportant, the case of laminar boundary layers is limited to the assumption that the temperature at the wall always attains the tank temperature T_m and satisfies the energy theorem within the boundary layer. This ties in also the assumption that temperature – and velocity – boundary layers are of equal thickness. Accurate calculations on flat plates indicate that this assumption also holds in a considerable supersonic range (reference 5).

The pressure in the y direction being constant, the density variation follows from the temperature variation as

$$\frac{T}{T_m} = 1 - \left(\frac{u}{w_m}\right)^2; \qquad \frac{\rho}{\rho_a} = \frac{T_a}{T} = \frac{1 - \left(\frac{u_a}{w_m}\right)^2}{1 - \left(\frac{u}{w_m}\right)^2} \tag{5.4}$$

The parameter for the boundary-layer characterization is derived from the known boundary conditions which for $u = v = 0$ in the boundary-layer equation leads to

$$\left(\frac{\partial \mu}{\partial y}\right)_w \left(\frac{\partial u}{\partial y}\right)_w + \mu_w \left(\frac{\partial^2 u}{\partial y^2}\right)_w = - \rho_a u_a \frac{du_a}{dx}$$

Since the internal friction is only dependent on T and no heat transfer takes place, $\left(\frac{\partial \mu}{\partial y}\right)_w = 0$, hence with application of δ

$$\lambda^* = - \left[\frac{\partial^2}{\partial\left(\frac{y}{\delta}\right)^2} \frac{u}{u_a}\right]_w = \frac{\rho_a \delta^2}{\mu_w} \frac{du_a}{dx} \tag{5.5}$$

We have avoided the introduction of the boundary-layer thickness itself in the equations other than at the unimportant place as upper limit of the integral. The version of (5.5) was largely taken from Walz's report (reference 4). The parameter λ^* differs from the conventional Pohlhausen parameter by the factor $\left(\frac{\delta^*}{\delta}\right)^2$, the density refers to that outside, the internal friction to that at the wall. For a class of velocity profiles, such as for $M = 0$, for instance, the individual profiles which are represented by the magnitude of parameter λ^* the quantities $\frac{\delta^*}{\delta}$ and $\left(\frac{\partial}{\partial \frac{y}{\delta}} \frac{u}{u_a}\right)_w$ can be taken as function of the parameter λ^* from the class of profiles, hence obtain $u_a \frac{d}{dx} \frac{\rho_a \delta^2}{\mu_w}$ by (5.2a) simply as function of λ^*. Choosing the Pohlhausen profiles as profile class gives the curve of Bohlen-Holstein (reference 3) in figure 1, while the Hartree or Howarth profiles result in Walz's curves of figure 1. Moreover, it is not necessary at all to have an analytical representation of the profile class, it can equally be given as family of experimental curves. If the outer flow is dependent on a Mach number, one profile class is used for each Mach number. In order not to come to grief because

of our ignorance in the sphere of compressible velocity profiles two known facts are taken advantage of: First, we know that the velocity profiles on the plate at constant pressure are not very closely related with the Mach numbers of the outer flow (reference 5). Therefore, this is assumed to be the case in retarded or accelerated flow also; secondly, we know that the single parametric method in the incompressible, which utilizes the Pohlhausen profiles, leads to fairly practical results, although the Pohlhausen profiles themselves do not represent the actual profiles very well. An exact representation of the velocity profiles themselves is not needed, the main point is the displacement thickness for which the integration over the profile form is already accomplished.

On the basis of these arguments we therefore select, independent of the Mach number, the Hartree profiles for the velocity distribution, which, as a rule, probably represent the incompressible boundary layer, best of all. The density variation is then given by (5.4) as function of the velocity distribution and owing to the presence of quantity $\frac{u_a}{w_m}$ as function of the Mach number.

By a numerical method the quantities $\frac{\delta^*}{\vartheta}$ and $\left(\frac{\partial}{\partial \frac{y}{\vartheta}} \frac{u}{u_a}\right)_w$ are then obtained as functions of λ^* and Ma, as exemplified for the following Ma which correspond to the $\frac{u_a}{w_m}$ values:

Ma	0	1	1.2	1.5	2.0
$\frac{u_a}{w_m}$	0	0.480	0.473	0.557	0.667

We obtain the curve system of figure 8.

The curves are shown at the left as far as the separation point, at the right they proceed to the point up to which the Hartree profiles are calculated. Several curves were extrapolated beyond it, and indicated by dashes. The curve Ma = 0 is identical with the Hartree curve from Walz.

Thus with the velocity distribution, the variation of the Mach number of the outer flow, and an initial value of $\frac{\rho_a \vartheta^2}{\mu_w}$ the parameter λ^* can be formed; with it and observing Ma the quantity

$u_a \frac{d}{dx} \frac{\rho_a \vartheta^2}{\mu_w}$ can be taken from figure 8 and the variation of $\frac{\rho_a \vartheta^2}{\mu_w}$ computed. From it we obtain again this quantity at a point shifted by one step and the calculation can then be repeated (reference 3). Although δ^* is wanted, it was preferred to compute $\frac{\rho_a \vartheta^2}{\mu_w}$ because the equation for this quantity is very much simpler. Knowing the outer flow, ϑ^2 can now be specified. To determine δ^* thus further requires $\frac{\delta^*}{\vartheta}$ which is a function of λ^* and Ma, represented in figure 9.

Since the quantity $\frac{d\delta^*}{dx}$ in the boundary-layer equation is to be defined as accurately as possible the following formula is of advantage

$$\frac{1}{\delta^*} \frac{d\delta^*}{dx} = \frac{\vartheta}{\delta^*} \frac{\partial}{\partial \lambda^*} \frac{\delta^*}{\vartheta} \frac{d\lambda^*}{dx} + \frac{\vartheta}{\delta^*} \frac{\partial}{\partial \frac{u_a}{w_m}} \left(\frac{\delta^*}{\vartheta} \right) \frac{d}{dx} \frac{u_a}{w_m}$$

$$+ \frac{1}{2} \left(\frac{1}{\frac{\rho_a \vartheta^2}{\mu_w}} \frac{d}{dx} \frac{\rho_a \vartheta^2}{\mu_w} + \frac{Ma^2}{u_a} \frac{du_a}{dx} \right) \tag{5.6}$$

This formula contains only quantities dependent either on Ma and λ^*, or which can be taken from the previous boundary-layer calculation. The derivative with respect to $\frac{u_a}{w_m}$, which is a function of Ma, was preferred over that with repect to Ma for reasons of simplicity. The first term at the right-hand side in (5.6) is generally the principle term.

If it is desired to eliminate $\frac{d\lambda^*}{dx}$ and $\frac{d}{dx} \frac{\rho_a \vartheta^2}{\mu_w}$ in (5.6) so as to secure $\frac{d\delta^*}{dx}$ merely in relation to $\frac{du_a}{dx}$, $\frac{d^2 u_a}{dx^2}$ (which then because of $\frac{d\lambda^*}{dx}$ enters in the equation) and coefficients solely dependent on λ^*, Ma, and Re, the expression becomes fairly long, but since this relationship is used later it is given here, the Re number being suitably referred to the outside density, the coefficient of friction at the wall and the displacement thickness:

$$Re^* = \frac{u_a \rho_a \delta^*}{\mu_w} \tag{5.7}$$

The formula reads

$$\frac{d\delta^*}{dx} = \frac{1}{Re^*}\left(\frac{\delta^*}{\vartheta}\right)^2\left(\frac{\partial}{\partial\frac{y}{\vartheta}}\frac{u}{u_a}\right)_w + \frac{\delta^*}{u_a}\frac{du_a}{dx}\left[2\left(\frac{\partial}{\partial\frac{y}{\vartheta}}\frac{u}{u_a}\right)_w\frac{\vartheta}{\delta^*}\frac{\partial}{\partial\lambda^*}\frac{\delta^*}{\vartheta} - \frac{\delta^*}{\vartheta} - 2 + Ma^2\right.$$

$$\left. + \frac{u_a}{w_m}\frac{\vartheta}{\delta^*}\frac{\partial}{\partial\frac{u_a}{w_m}}\frac{\delta^*}{\vartheta}\right] + \left(\frac{\vartheta}{\delta^*}\right)^3\frac{\partial}{\partial\lambda^*}\frac{\delta^*}{\vartheta}Re^*\left[\frac{\delta^{*2}}{u_a^2}\frac{d^2u_a}{dx^2}\right.$$

$$\left. - \left(\frac{\delta^*}{u_a}\frac{du_a}{dx}\right)^2\left(2\frac{\delta^*}{\vartheta} + 4 - Ma^2\right)\right]$$

$$= \frac{\alpha_1}{Re^*} - \alpha_2\frac{\delta^*}{u_a}\frac{du_a}{dx} - \alpha_3 Re^*\frac{\delta^{*2}}{u_a}\frac{d^2u_a}{dx^2} - \alpha_4 Re^*\left(\frac{\delta^*}{u_a}\frac{du_a}{dx}\right)^2 \qquad (5.8)$$

It contains the first and second derivative of u_a made dimensionless with the displacement thickness and the outside velocity, and also Re^* and coefficients that are dependent on λ^* and Ma.

The coefficients α_1, α_2, and α_3 for $\lambda^* = 0$ are given in the following table:

TABLE II

LAMINAR BOUNDARY LAYER; $\lambda^* = 0$

Ma	0	1	1.2	1.5	2.0
$\frac{u_a}{w_m}$	0	0.408	0.473	0.557	0.667
α_1	1.47	2.02	2.30	2.76	3.82
α_2	5.61	4.89	4.60	3.87	2.37
α_3	0.349	0.284	0.256	0.219	0.154

Later on the equation is to be applied to the case where the velocity distribution differs little and monotonically from $u_a = \text{Const}$, so that $\frac{\delta^*}{u_a}\frac{du_a}{dx}$ and $\frac{\delta^{*2}}{u_a}\frac{d^2u_a}{dx^2}$ are also regarded as

being small. Restricted to the linear terms in the derivatives of u_a, the term with α_1 can be struck out and the coefficients α_2 and α_3 taken at the point $\lambda^* = 0$ for the specified Mach number. The dependence of α_1 on the derivatives of u_a proves to be so small that the same can be done for this quantity too.

So on the assumption of small derivatives of u_a simply (5.8) is taken with the constants of table II for the corresponding Ma, for $\frac{d\delta^*}{dx}$ of a laminar boundary layer.

To obtain a formula for the variation of the displacement thickness of a turbulent boundary layer a different procedure is required. On analyzing the cause of the variation of an incompressible turbulent velocity profile at a specific pressure variation it is found that the pressure forces are primarily responsible. The shearing stresses introduced by the turbulent intermingling play, however, a subordinate part. It is true that the difference of the two effects is not so far reaching that a second profile could be computed accurately enough from the specified velocity profile when the shearing stresses are discounted, because the shearing stresses are able to substantially modify the character of the profile; but for the calculation of the variation of displacement thickness, which essentially involves an integral over the velocity variation in the incompressible case, the shearing stresses can be disregarded.

The result at $Ma = 0$ is the following approximation formula for the turbulent boundary layer:

$$\frac{d\delta^*}{dx} = -\frac{\delta^*}{u_a}\frac{du_a}{dx}\int_0^{\delta}\left[\left(\frac{u_a}{u}\right)^2 - \frac{u}{u_a}\right] d\frac{y}{\delta^*} \qquad (5.9)$$

As the integrand is always positive, it can be taken from this formula that a speed increase is accompanied by a decrease in displacement thickness and a speed decrease by an increase in displacement thickness. At constant outside velocity the displacement thickness remains constant, according to (5.9). This result is naturally wrong, as indicated by experiments on the plate at constant pressure. For in this case the variation in displacement thickness is contingent upon the turbulent shearing stresses, so no correct result is to be expected. The formula could be improved by the addition of the conventional formula for the variation of

the displacement thickness, but it would serve no useful purpose, as will be seen. It is of greater significance that in contrast to equation (5.8) for the laminar boundary layer the second derivative of u_a is lacking in (5.9). Since (5.9) was obtained by several rougher omissions its practicability is illustrated in figure 10. The experimental values of $\frac{1}{u_a}\frac{du_a}{dx}$ and $\frac{d\delta^*}{dx}$ are shown plotted against the arc length x of Gruschwitz's (reference 6) test series 3, along with the variation in displacement thickness calculated by (5.9), the integral being formed at $\frac{du_a}{dx} = 0$. It is found that the formula reproduces the actual conditions adequately, as far as the area of greater accelerations, where errors begin to be introduced. This is, of course, due to the fact that $\delta^* = 0$ imposes a limit on the decrease in displacement thickness.

These experiences in the incompressible zone can now be interpreted to the effect that the turbulent shearing stresses for the calculation of $\frac{d\delta^*}{dx}$ can also be cancelled in the compressible zone. But even this assumption is insufficient to develop a law for the variation in displacement thickness; additional data on the density distribution in the boundary layer are needed. In the case of turbulent boundary layers the energy theorem is not directly applicable, because the density-boundary layer is probably twice as great as the velocity-boundary layer; hence, the density varies in an area in which the velocity is already practically considered constant (fig. 11). The result of it is that the variation in density plays the same role in the calculation of δ^* as the variation in speed within the boundary layer. Unfortunately only one measurement of a turbulent supersonic profile is available, and naturally there is little sense in developing a theory without further basis. However, in order to reach a tolerably correct numerical value, the part of the boundary layer in which the density alone varies is disregarded for the present, since it involves only about 10 percent of the displacement thickness, and, in the remaining portion, putting the stream density as a function of the velocity as follows:

$$\frac{\rho u}{\rho_a u_a} = H\left(\frac{u}{u_a}\right) \tag{5.10}$$

H to be taken from the experiment. Now the derivatives of ρ can be expressed by derivatives of u, u_a, and ρ_a with the aid of (5.10). This enables us to derive a formula for the variation of displacement thickness, neglecting the turbulent shearing stresses.

$$\frac{d\delta^*}{dx} = -\frac{\delta^*}{u_a}\frac{du_a}{dx}\left[1 - Ma^2 + \int_0^{\delta}\frac{\rho_a}{\rho}H'\left(\frac{\rho_a u_a^2}{\rho u^2} - 1\right)d\frac{y}{\delta^*}\right]$$

$$= -\alpha_2\frac{\delta^*}{u_a}\frac{du_a}{dx} \qquad (5.11)$$

H' is the derivative of the function H according to the argument $\frac{u}{u_a}$ and δ the place where $\frac{u}{u_a}$ can be put equal to unity $\left(\frac{u}{u_a} = 1\right)$, while δ^* represents the correct displacement thickness hence, integrate up to a point where $\frac{p}{p_a}$ itself is equal to unity $\left(\frac{p}{p_a} = 1\right)$. This means, we state that the 10 percent of the displacement thickness between the point $\frac{u}{u_a} = 1$ and $\frac{p}{p_a} = 1$ contributes to the variation of the displacement thickness an amount which corresponds to its portion of the displacement thickness. For $Ma = 0$, equation (5.11) naturally changes to (5.9). If the density and speed in the boundary layer are specified, the integral can be evaluated also. We have calculated the expression in parentheses for a profile by Gruschwitz, for which $\frac{du_a}{dx} = 0$, and for the velocity and density profile represented in figure 11; thus we obtain the constant α_2 for two values of the Mach number.

TABLE III

TURBULENT BOUNDARY LAYER

Ma	0	1.7
α_2	5.1	2.2

The close agreement of coefficient α_2 for the turbulent and the laminar velocity profile is noteworthy.

6. STABILITY STUDY ON THE FLAT PLATE

A study of the equilibrium of boundary layer and supersonic flow on the flat plate indicates that an unstable state is involved. The growth of a small disturbance in a laminar boundary layer differs somewhat from that in a turbulent layer and is, especially in the last

case, very rapid. In incompressible flow a stable equilibrium exists between principal flow and boundary layer.

Having secured the variation of displacement thickness δ^* in relation to the velocity variation of the outer flow, the reciprocal effect of principal - and boundary layer flow is now analyzed in the simplest case, namely, in the flow at the plate without specified pressure distribution.

Since the effect of small disturbances is to be involved, the Mach number of the outer flow Ma is regarded as constant and the v component of the velocity considered small relative to the velocity of sound. After introduction of a velocity potential the simple equation (2.2) is involved, and written in the form

$$\Phi_{yy} = \Phi_{xx} (Ma^2 - 1) \tag{6.1}$$

The x-axis is to be in plate direction, the y-axis normal to it.

Now it is necessary to represent the effect of the boundary layer on the potential flow in form of a boundary condition. The boundary layer is therefore visualized as being replaced by an elastic layer superimposed on the plate, which has the property of always attaining the thickness equivalent to the displacement thickness of the boundary layer at the particular place for the prevailing velocity distribution. That is, the equation

$$v = u \frac{d\delta^*}{dx} \tag{6.2}$$

must be satisfied for $y = \delta^*$.

This condition is inconvenient to the extent that the boundary for which it is to be fulfilled is not specified beforehand. But, inasmuch as the disturbances are to be small, hence the outerflow is to differ very little from a flow $u_a = \text{Const.}$, the boundary condition for displacement thickness δ^* in undisturbed flow is assumed. By assumption the departure of δ^* from the value of the displacement thickness for the undisturbed flow must be small. Hence it seems immaterial whether v is specified at $y = \delta^*$ or at $y = \delta^* + d\delta^*$ in the linearized problem. Besides, the study is to be restricted to such a small area that $\frac{d\delta^*}{dx}$ itself can be regarded as constant at $u_a = \text{Const.}$

Furthermore the boundary condition (6.2) has the property of giving the same v component of the velocity at $y = \delta^*$ as a boundary layer with equal $\frac{d\delta^*}{dx}$, on the assumption of potential flow in the entire space.

In (6.2), v and u are none other than the components of the outer velocity, hence in the notation of the preceeding section equal to v_a and u_a.

Applying (5.8) or (5.11) to $\frac{d\delta^*}{dx}$ gives then as boundary condition of the problem, linearized in the derivatives of u, the following equation for

$$y = \delta^*: \quad v = u \frac{\alpha_1}{Re^*} - \alpha_2 \delta^* \frac{\partial u}{\partial x} - \alpha_3 Re^* \frac{\partial^2 u}{\partial x^2} \delta^{*2} \tag{6.2a}$$

If a laminar flow is involved the corresponding constants must be taken from table II; if, turbulent flow, table III; in the latter case, α_3 must be put = 0. In view of the linearization δ^* and Re^* must also be regarded as constant; although the variation of u in the first term is not important, it is considered nevertheless, because the solution then is reduced to the treatment of a homogeneous linear differential equation, which means some simplification.

Now it is attempted to find the solution for the case that the plate is exposed to a flow with the velocity $u(x,y) = u_o = \text{Const}$ and at a point $x = 0$ at the plate the velocity is artificially varied by an amount $\bar{u} \ll u_o$. The coordinate system is turned through a small angle so that the x-axis in point $x = 0$ is exactly in flow direction and the y-axis normal to it. The tangent of the angle of rotation is defined by the variation of the displacement thickness at $x = y = 0$, which is equal to

$$\frac{d\delta^*}{dx} = \frac{\alpha_1}{Re^*}$$

Strictly speaking a transformation of the coordinates in the equations themselves should be effected. But since the boundary layer itself makes no difference between these two directions, and so a rotation merely involves more paper work without any physical significance, it is disregarded and the equations applied to the new coordinates. The coordinates are in addition visualized as being made dimensionless by the displacement thickness and the origin shifted to the point $x = 0$, $y = \delta^*$.

These new coordinates are denoted with

$$x' = \frac{x}{\delta^*};\ y' = \frac{y - \delta^*}{\delta^*}$$

and after introducing the velocity potential in (6.2a) give the following differential equation with the respective boundary condition

$$\Phi_{y'y'} = \Phi_{x'x'}\,(Ma^2 - 1) \tag{6.1a}$$

at

$$y' = 0;\ \Phi_{y'} = -\alpha_2\Phi_{x'x'} - a_3 Re^*\Phi_{x'x'x'} \tag{6.2b}$$

Assuming a very general solution of (6.1a), and writing the potential as sum of a potential of a principal flow u_o and a small disturbance

$$\Phi = u_o\delta^*x' + \bar{u}\delta^*\left[f\left(x' - \sqrt{Ma^2 - 1}\,y'\right) + g\left(x' + \sqrt{Ma^2 - 1}\,y'\right)\right]$$

f and g are arbitrary functions of which it is merely required that their sum at $x' = y' = 0$ be equal to unity. It is seen that g gives Mach lines which point toward the boundary layer, hence stem from a disturbance from the outside. This function is thus put identically zero since such disturbances are to be disregarded. Introduction of the thus obtained solution in the boundary condition gives the functional form of f. Denoting the derivative with respect to the argument

$$\eta = x' - \sqrt{Ma^2 - 1}\,y'$$

with subscript η, we get

$$\Phi_{x'} = u_o\delta^* + \bar{u}\delta^*f_\eta;\quad \Phi_{x'x'} = \bar{u}\delta^*f_{\eta\eta};$$

$$\Phi_{x'x'x'} = \bar{u}\delta^*f_{\eta\eta\eta};\quad \Phi_{y'} = -\bar{u}\delta^*\sqrt{Ma^2 - 1}f_\eta$$

which inserted in (6.2b) gives an ordinary differential equation of the form

$$\alpha_3 Re^*f_{\eta\eta\eta} + \alpha_2 f_{\eta\eta} - \sqrt{Ma^2 - 1}\,f_\eta = 0 \tag{6.3}$$

This equation is easily solved. First postulating a laminar boundary layer, hence $\alpha_3 \neq 0$. Then from the requirement for $x' = y' = 0$: $f = 1$, a requirement for the second derivative $f_{\eta\eta}$ can be satisfied, because the upper equation can be regarded as differential equation of the second order of f_η. Since at this point only the consequences of small velocity disturbances, not the consequences of disturbances of the velocity difference are to be studied, the added requirement for $x' = y' = 0$ is $f_{\eta\eta} = 0$, which gives the solution

$$f_\eta = \frac{t_1}{t_1 - t_2} e^{t_2\eta} - \frac{t_2}{t_1 - t_2} e^{t_1\eta}$$

where t_1 and t_2 are abbreviations for the expressions

$$t_{1,2} = -\frac{1}{2}\frac{\alpha_2}{\alpha_3 Re^*} \pm \sqrt{\frac{1}{4}\left(\frac{\alpha_2}{\alpha_3 Re^*}\right)^2 + \frac{\sqrt{Ma^2 - 1}}{\alpha_3 Re^*}} \qquad (6.4)$$

As Re^* in general has the order of magnitude of 10^3, the last term under the root is a term of greatest influence. Thus for appraisals at high Re^* we can put

$$t_{1,2} \approx \pm\sqrt{\frac{\sqrt{Ma^2 - 1}}{\alpha_3 Re^*}} \qquad (6.4a)$$

It is to be noted however that the critical Re^* which corresponds to a value of about 1.4×10^3 must not be exceeded as will be shown later.

By use of (6.4) the velocity distribution in a laminar boundary layer on the plate is obtained as:

$$u = \frac{1}{\delta^*}\Phi_{x'} = u_o + \frac{\bar{u}}{t_1 - t_2}\left[t_1 e^{t_2\left(x' - \sqrt{Ma^2 - 1}\, y'\right)} - t_2 e^{t_1\left(x' - \sqrt{Ma^2 - 1}\, y'\right)}\right] \qquad (6.5)$$

which by (6.4a) is reduced to the simple form

$$u \approx u_o + \bar{u}\cosh\sqrt{\frac{\sqrt{Ma^2 - 1}}{\alpha_3 Re^*}}\left(x' - \sqrt{Ma^2 - 1}\, y'\right) \qquad (6.5a)$$

If a turbulent boundary layer were involved, hence $\alpha_3 = 0$, the first summand in (6.3) cancels out and only one boundary condition can be satisfied. Again requiring $f = 1$ for $x' = y' = 0$ gives

$$f_\eta = e^{\frac{\sqrt{Ma^2-1}}{\alpha_2}\eta}$$

The velocity field under the assumption of a turbulent boundary layer at the plate is

$$u = u_o + \bar{u}e^{\frac{\sqrt{Ma^2-1}}{\alpha_2}\left(x' - \sqrt{Ma^2-1}y'\right)} \tag{6.6}$$

From (6.5) and (6.6) it is seen that the boundary disturbance along Mach lines is propagated into the flow. The interference velocity $\bar{u}$ is always accompanied by a function which grows considerably with rising value of the argument, while in the case of the laminar boundary layers the coefficient α_3 plays the principal part. In turbulent boundary layers the coefficient α_2 is essentially involved. Thus the boundary layer of a flat plate in flow with constant velocity is in both instances in an unstable state of equilibrium with the principal flow, which with observance of the terms of the first order only, lets a small disturbance grow infinitely. The type of growth is, of course, quite dissimilar on the two boundary layers. To secure a measure for the instability of the state, we may ask for which value of $x' = \frac{x}{\delta^*}$ at $y' = 0$ the disturbance has grown to twice the amount and call this quantity the length of growth A. It is not made dimensionless by the displacement thickness.

The length of growth in a laminar boundary layer A_l is assessed by (6.5a). The hyperbolic cosine grows for a value of the argument of around 1.3 to the amount 2. Accordingly

$$A_l \approx 1.3\sqrt{\frac{\alpha_3 \bar{R}e^*}{\sqrt{Ma^2 - 1}}}\,\delta^* \tag{6.7}$$

The length of growth of a turbulent boundary layer A_t is

$$A_t = 0.70\,\frac{\alpha_2}{\sqrt{Ma^2 - 1}}\,\delta^* \tag{6.8}$$

Postulating a laminar boundary layer at $Re^* = 1000$, tables II and III give the following length of growth

TABLE IV

Ma	1.2	1.5	1.7	2.0
$\frac{A_l}{\delta^*}$	25	18		12
$\frac{A_t}{\delta^*}$			1.1	

Noteworthy is the unusually short length of growth in the turbulent boundary layer; but even that in the laminar layer is still very small when bearing in mind that the displacement thickness in supersonic flows is of the order of magnitude of 10^{-3} to 10^{-2} centimeters.

The investigation was restricted to small disturbances. The extent of growth once they have reached greater amounts remains to be proved. One thing is certain that the outerflow cannot increase to great velocities, because the boundary layer cannot drop below the amount $\delta^* = 0$. Thus no limit in velocity decrease is imposed. It may be presumed that the velocity decreases until the boundary layer breaks away. In general, the instability of the discussed equilibrium condition will become evident in a pressure rise, probably an oblique compressibility shock. It would not be surprising if oblique compressibility shock occurred in the center on a flat wall (fig. 7(a)). The example cited here could be multiplied by many others, perhaps even by flow around conical tips. It should be kept in mind that a pressure rise can cause transition of the boundary layer. In the example adduced here the boundary layer is already certainly turbulent.

This study of plate flow can be regarded as first result in this sphere of instability of supersonic boundary layers. It would be desirable to get away from the assumption of small disturbances and constant flow velocity. This seems altogether possible by a combination of characteristics method and boundary layer computation. For the turbulent boundary layer, of course, the laws of variation δ^* would have to be analyzed first.

One unusual fact is that in the measured pressure distribution on a wing, such as those by Göthert (reference 7), for instance, pressure increases were almost never observed in the supersonic zone, except in form of compressibility shock or occasionally at small Reynolds numbers, where laminar boundary layers must be assumed.

It appears entirely possible that this fact might be explainable by the cited properties of the supersonic boundary layer.

The corresponding behavior of a laminar boundary layer in incompressible flow (Ma = 0) is briefly indicated. The disturbance at great distances from the wall, that is, for great values of y, must disappear. On these premises, (6.1a), (6.2b) by the same method of calculation give

$$u = u_o + ue^{-\beta_1 x' - \beta_2 y'} \cos(\beta_2 x' - \beta_1 y') \tag{6.9}$$

with the abbreviations

$$\beta_1 = \frac{1}{\alpha_3 Re^*}\left\{\frac{\alpha_2}{2} + \sqrt{\frac{1}{2}\left[\sqrt{\left(\frac{\alpha_2}{2}\right)^4 + (\alpha_3 Re^*)^2} + \left(\frac{\alpha_2}{2}\right)^2\right]}\right\}$$

$$\beta_2 = \frac{1}{\alpha_3 Re^*}\sqrt{\frac{1}{2}\left[\sqrt{\left(\frac{\alpha_2}{2}\right)^4 + (\alpha_3 Re^*)^2} - \left(\frac{\alpha_2}{2}\right)^2\right]}$$

The decisive term at high Re* numbers is again $\alpha_3 Re^*$. For Re* = 500 it approximately is

$$\beta_1 \approx \beta_2 \approx \frac{1}{\sqrt{2\alpha_3 Re^*}} \approx 0.053$$

that is, a strongly damped oscillation is involved. The analyzed equilibrium of laminar boundary layer and outer flow in the subsonic zone is extremely stable according to it. This method of analyzing offers the further possibility of exploring the stability of laminar subsonic boundary layer relative to nonstationary disturbances and comparing the results with Tollmien's calculations (reference 8). For nonstationary velocity variations Pohlhausen's method is, of course, not practical in general, in the form given here.

Incidentally, the requirement of damping of the disturbance for great y is not fulfillable in subsonic flow on the assumption of a turbulent boundary layer at the plate. This result may have its cause in the fact that (5.9) does not meet all requirements.

7. SIGNIFICANCE OF BOUNDARY LAYER IN THE PRESSURE DISTRIBUTION ON A BODY

Appraisals indicate that the flow in the critical range of sonic velocity is very substantially affected by the boundary layer. Without its inclusion a correct calculation of the pressure distribution therefore seems, in general, not very promising. In many instances the behavior of the boundary layer actually governs the pressure distribution.

On examining the pressure distribution at a bump computed in section 3, (fig. 4), a symmetrical velocity distribution is also found on a body symmetrical about the y-axis. This is, however, in great contrast to the experience in tests (compare, fig. 12), where symmetrical peaks were invariably accompanied by asymmetrical velocity distributions. Naturally the question is whether there is only one solution for each bump but it will be shown that, owing to the boundary-layer effect, symmetrical solutions can be expected as little as in the example of the velocity distribution in a nozzle (fig. 7(b)).

By (5.8) the displacement thickness of a laminar boundary layer for constant outer speed is

$$\delta^* = \sqrt{2\alpha_1 \frac{\mu_w}{u_a \rho_a x}}$$

What is the possible extent of the bump in order that the boundary layer remain laminar? Figuring with tests in a low-pressure tunnel, the values at critical velocity are

$$u_a = 3 \times 10^4 \text{cm/sec}; \quad \rho_a = \underset{\text{CGSE}}{0.8 \times 10^{-3}} \text{g/cm}^3; \quad \mu_w = 1.8 \times 10^{-4}$$

It is to be presumed that the critical Reynolds number at sonic velocity does not differ substantially from that in incompressible flow. Taking the critical Reynolds number formed with the plate length at

$$\text{Re}_{\text{crit.}} = 5 \times 10^5$$

gives the critical Reynolds number (5.7) formed with the displacement thickness at

$$Re^*_{crit.} = 1.4 \times 10^3$$

with the previous values of u_a, ρ_a, and μ_w the critical values of plate length and displacement thickness are

$$x_{crit.} = 3.8 \text{ cm}; \quad \delta^*_{crit.} = 1.1 \times 10^{-2} \text{ cm}$$

So in order to prevent transition from laminar to turbulent flow in the boundary-layer model, lengths of only a few centimeters may be permitted in the usual test arrangements, provided that no strong accelerations are involved.

Conversely, the critical length indicated here gives a measure for when the transition point is to be expected on a plate flow in an exhaustion tunnel at sonic velocity. In a free-air test this length is reduced by about half because of the higher density.

In the schlieren photograph of an infantry shell in flight at around sonic velocity (fig. 13) (references 9 and 10) the oblique compressibility shock is evidently released by transition, its effect being probably amplified by the unstable behavior of the boundary layer. The fact that a missile at small supersonic speed is involved is immaterial; since a straight compressibility shock prevails in front of nose of the missile, it actually flies as if in a subsonic flow.

Analyzing the bump in figure 4, which at the point of its greatest height has nearly constant sonic velocity for some distance, and supposing the points of strong velocity rise and velocity decrease ($x = 0.6$) to be about 2 centimeters apart, the displacement thickness at the peak is certainly greater than that of a plate 1 centimeter in length in flow at sonic velocity. Therefore

$$\delta^*_{x=0} > 0.56 \times 10^{-2} \text{ cm}$$

At the point of substantial speed decrease, separation must be definitely expected. A calculation by the expanded Pohlhausen method shows that the momentum thickness grows with increasing arc length. Much greater is the rise in the ratio of displacement thickness to momentum thickness (fig. 9) which for $Ma = 1$ increases

from point $\lambda^* = 0$ to the separation point from value 3.2 to 4.7. Considering the fact that the momentum thickness itself increases up to the separation point, an empirical rule can be established according to which the displacement thickness is doubled between $\lambda^* = 0$ and the point of separation.

The difference between the displacement thickness at the separation point and at the highest point of the peak is in the example; therefore

$$\delta^*_{separ.} - \delta^*_{x=o} \approx 0.56 \times 10^{-2} \text{ cm}$$

The difference in height of the highest point and at point of separation $h_{separ.}$ is (compare fig. 4)

$$h_{separ.} \approx 3 \times 10^{-2} \text{ cm}$$

While the variation in $h_{separ.}$ due to the boundary-layer effect amounts to a mere 20 percent, the illustration shows that a change in height of bump by this amount must be followed by an extraordinarily great change in velocity distribution, so that there can be no question of attaining symmetrical results in the experiment.

The conditions in the presence of a turbulent boundary layer are considerably worse. A little calculation on Grushwitz's test series 3 (reference 6) discloses that the displacement thickness multiplies from the point of transition to the point of turbulent separation by about 25 times. Assuming turbulent separation at the point of severe velocity drop the greatest displacement effect (height of bump + displacement thickness) would also exist on a bump of considerably greater absolute dimensions at the point of separation due to boundary-layer growth. It is supposed that the displacement effect of the body, increased by the displacement effect of the boundary layer, undergoes no substantial increase behind the highest point of the bump. In turbulent boundary layer and thin profiles or low bumps this is possible only to the extent that a compressibility shock occurs at the point of greatly reduced profile thickness; furthermore, a compressibility shock would have to occur so much farther downstream as the bump or the profile is flatter. It also is feasible that the effect of the increase in displacement thickness is raised by strong return flow behind the point of separation. These qualitative results can be checked against the work of Göthert (reference 7).

The fact that a compressibility shock can occur when there is enough space available for the increased displacement thickness caused by it is to be regarded as reason for the fact that the separation computed by stream filament theory in figure 7(b) is almost exactly coincident with the start of the compressibility shock in the test.

It may be asked how the streamline pattern in a flow problem must look, in order that the compressibility shock be possible. This can be answered to the effect that the compressibility shock on slender bodies is to be expected near the point of vanishing streamline curvature. Since the streamlines in the zone of critical sonic velocity are approximately parallel, the points of vanishing streamline curvature must lie near a common orthogonal trajectory, hence, a potential line. Along it the velocity changes little according to (1.8). In a flow that differs little from the critical sonic velocity, the free-stream velocity is therefore to be expected in the vicinity of points with zero streamline curvature. If the curve decreases rapidly at a place with supersonic velocity a decrease to the outer velocity must be counted on. The marked velocity variations in figure 4 coincide with the streamline inflection points. On flat profiles a point of separation can be regarded as starting point of a free streamline with very little curvature. The streamline curvature must thus decrease very substantially in the separation point and it is seen that a strong compressibility shock produces through the separation connected with it a streamline pattern that favors the appearance of the compressibility shock. This argument is therefore not suitable for finding the location of a compressibility shock.

8. CONCLUDING REMARKS

The preceeding work shows that in a calculation conforming to reality the pressure distribution of a body in a flow at supercritical free-stream velocity may not be given by the potential flow, that the boundary layer plays a decisive role here. In general, the potential flow around the body permits not even an approximate calculation of the boundary layer. This means that in contrast to incompressible flow the pressure distribution on flat bodies can also be much different.

It is therefore intended to first improve the process of calculation of the potential flow with a supersonic region. With the process we will ascertain the flow around a substitute body. This will have approximately the same displacement effect that is found on an experimentally investigated body including its deadwater region and

the displacement effect of its boundary layer. We can also anticipate from our calculation a strong velocity increase at the body nose and a strong velocity decrease at the point where the curvature of the substitute body disappears.

Translated by J. Vanier
National Advisory Committee
for Aeronautics

REFERENCES

1. Stanton, T. E.: Velocity in a Wind Channel Throat. Aeron. Res. Comm. R. & M., No. 1388.

2. Oswatitsch, Kl., and Rothstein, W.: Das Strömungsfeld in einer Lavaldüse. Vorabdr. d. Jahrb. 1942 d. deutsch. Luftfahrtforsch. in den Techn. Ber. Heft 5, Oct. 15, 1942.

3. Holstein, H., and Bohlen, T.: Verfahren zur Berechnung laminarer Grenzschichten. Lilienthal-Ges. f. Luftfahrtforschung Bericht S 10 (Preisausschreiben 1940.), p. 5.

4. Walz, A.: Ein neuer Ansatz für das Geschwindigkeitsprofil der laminaren Reibungsschicht. Lilienthal-Ges. f. Luftfahrtforschung Bericht 141.

5. Hantzsche, W., and Wendt, H.: Zum Kompressibilitätseinfluss bei der laminaren Grenzschicht der ebenen Platte. Jahrb. 1940 d. deutsch. Luftfahrtforsch. I, p. 517.

6. Gruschwitz, E.: Die turbulente Reibungsschicht in ebener Strömung bei Druckabfall und Druckanstieg. Ing.-Arch., II. Bd., 1931, p. 321.

7. Göthert, B., and Richter, G.: Messung am Profil NACA 0015-64 im Hochgeschwindigkeitskanal der DVL, FB 1247.

   Göthert, B.: Druckverteilungs- und Impulsverlustschaubilder für die Profile NACA 0006-1, 130, usw. bei hohen Unterschallgeschwindigkeiten. FB 1505/1-5.

8. Tollmien, W.: Ein allgemeines Kriterium der Instabilität laminarer Geschwindigkeitsverteilungen. Nachr. d. Ges. d. Wiss. zu Göttingen, Math.-phys. Kl., Fachgr. I, Math., Neue Folge, Bd. I, Nr. 5, 1935, p. 79.

9. Cranz, C.: Lehrbuch der Ballistik, Bd. II, p. 452, Fig. 22.

10. Ackeret, J.: Gasdynamik. Handb. d. Physik, Bd. VII, p. 338.

11. Busemann, A.: Das Abreissen der Grenzschicht bei Annäherung an die Schallgeschwindigkeit. Jahrb. 1940 d. deutsch. Luftfahrtforschung I, p. 539.

12. Frössel, W.: Experimentelle Untersuchung der kompressiblen Strömung an und in der Nähe einer gewölbten Wand, 1. Teil. UM 6608 (Abb. 12 entstammt einem nicht veröffentlichten Vorversuch).

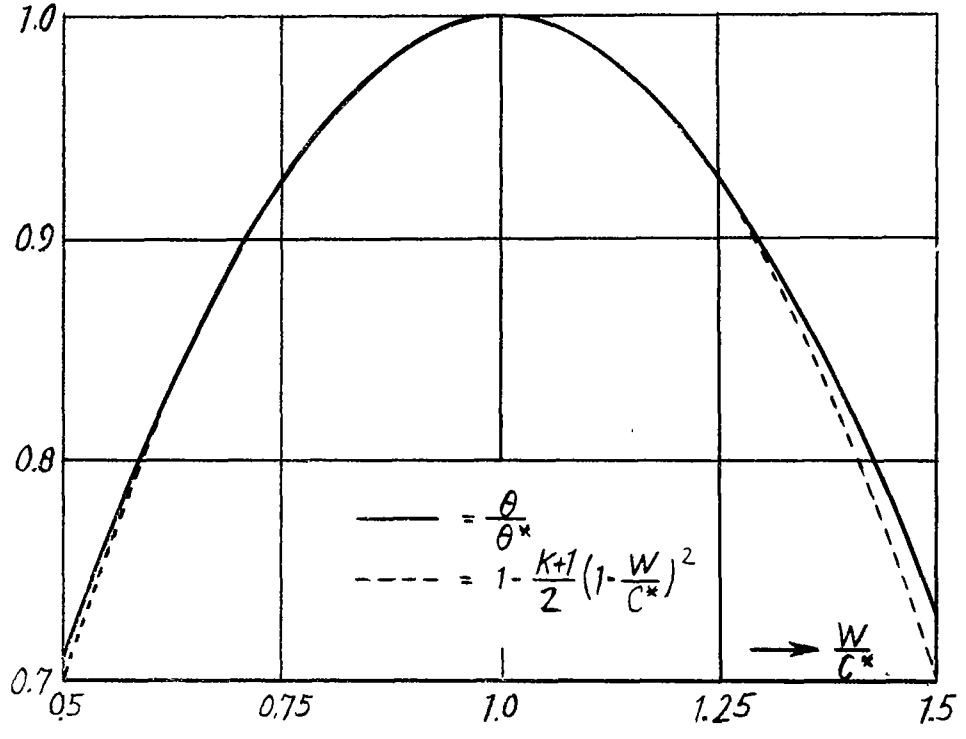

Figure 1.- Relationship between stream density θ/θ^* and velocity w/c^* with approximation parabola for $w \approx c^*$.

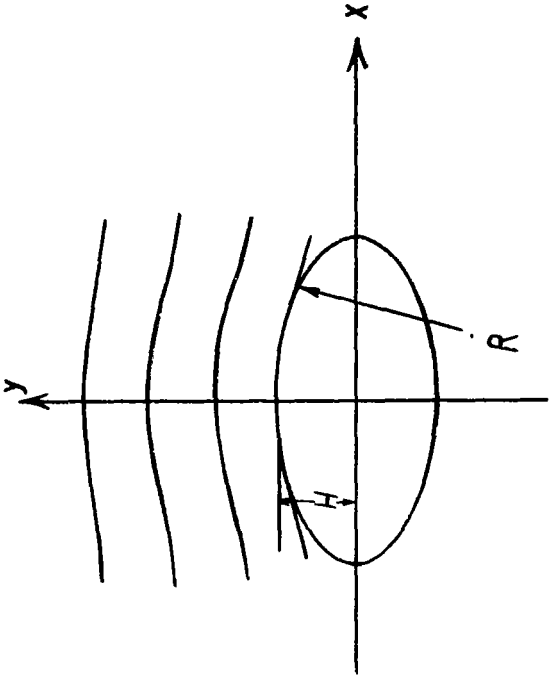

Figure 2.- Field of flow.

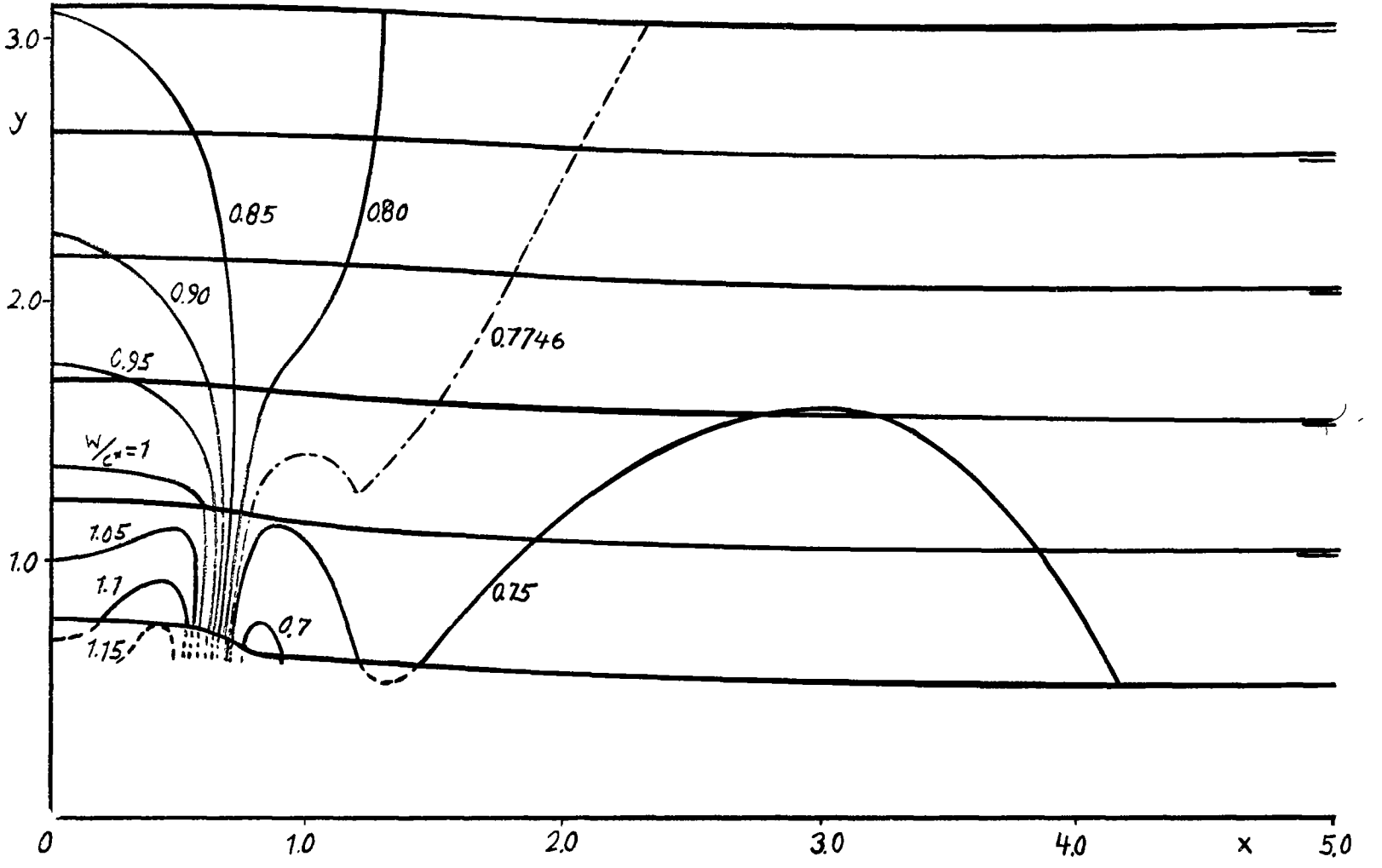

Figure 3.- Streamlines and contours of equal velocity of a flow with supersonic zone (-.-.- contour free stream velocity).

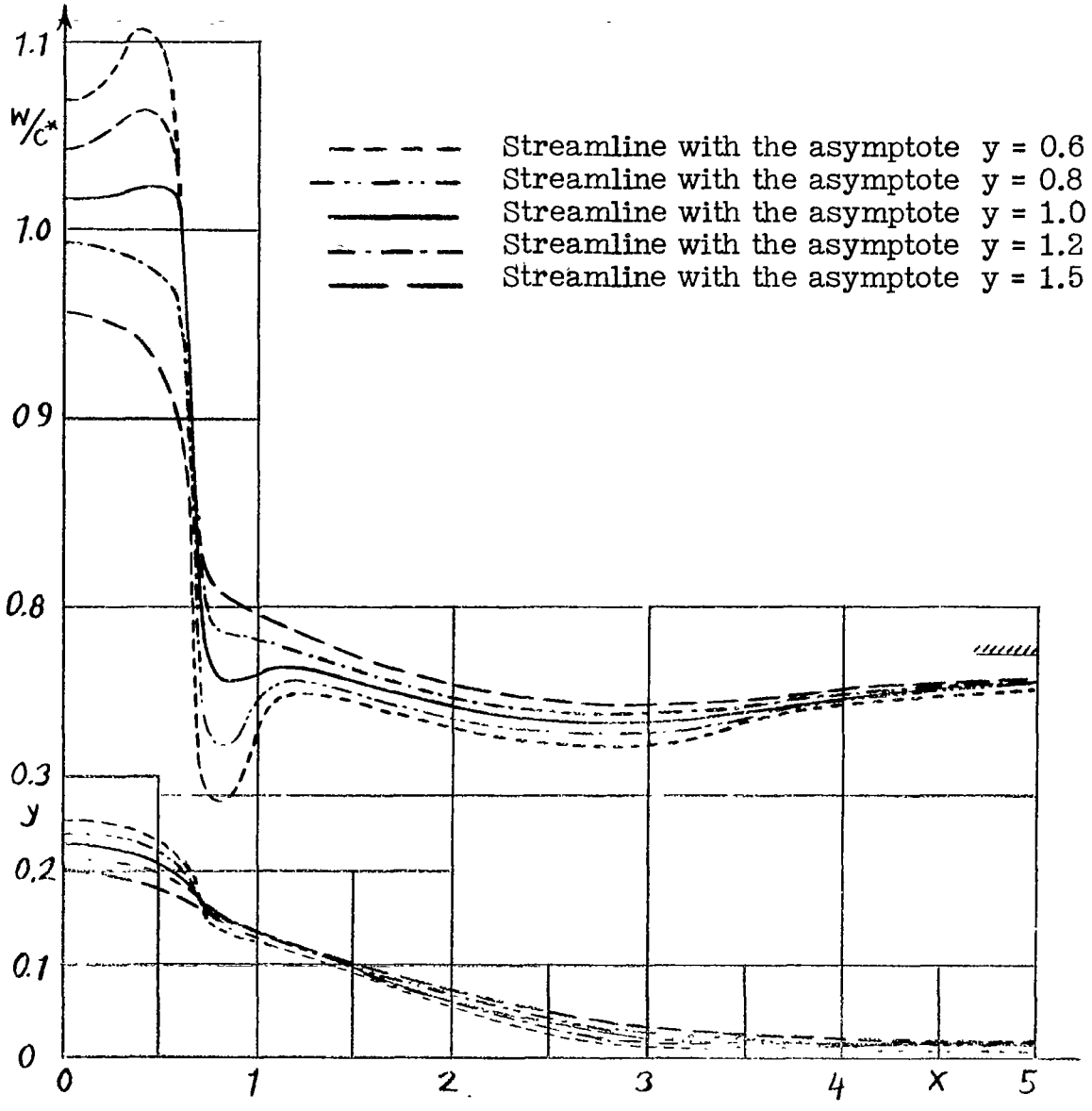

Figure 4.- Velocity distributions over various bumps.

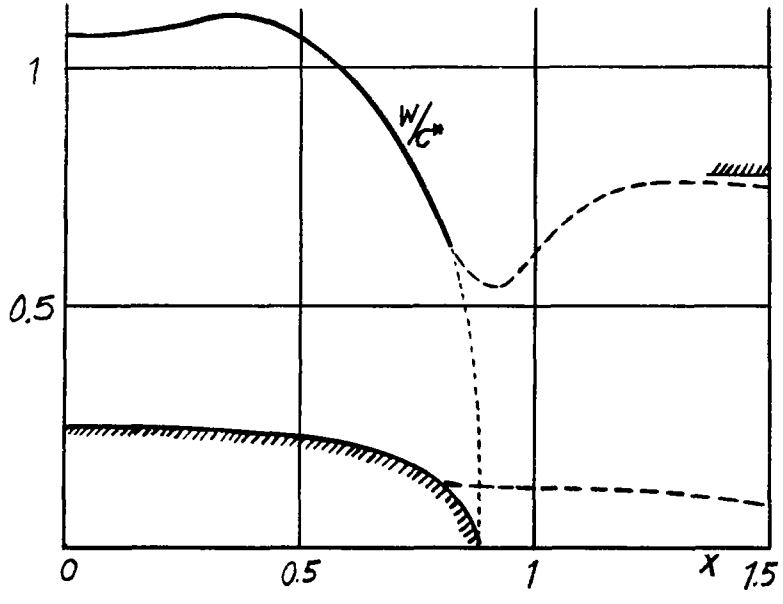

Figure 5.- Velocity distributions along a body with local supersonic zone (extrapolated near stagnation point).

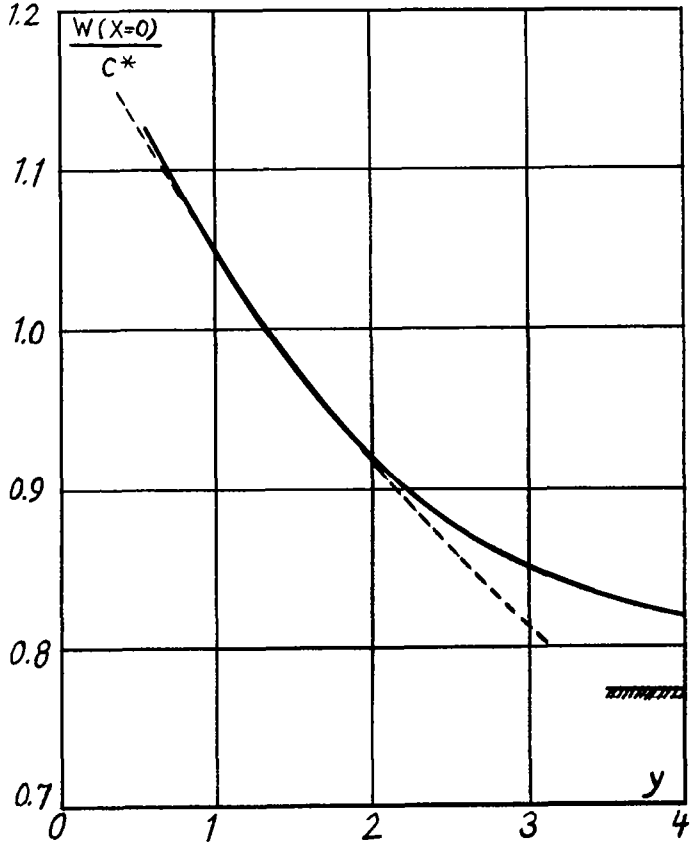

Figure 6.- Velocity distributions on axis x = 0.

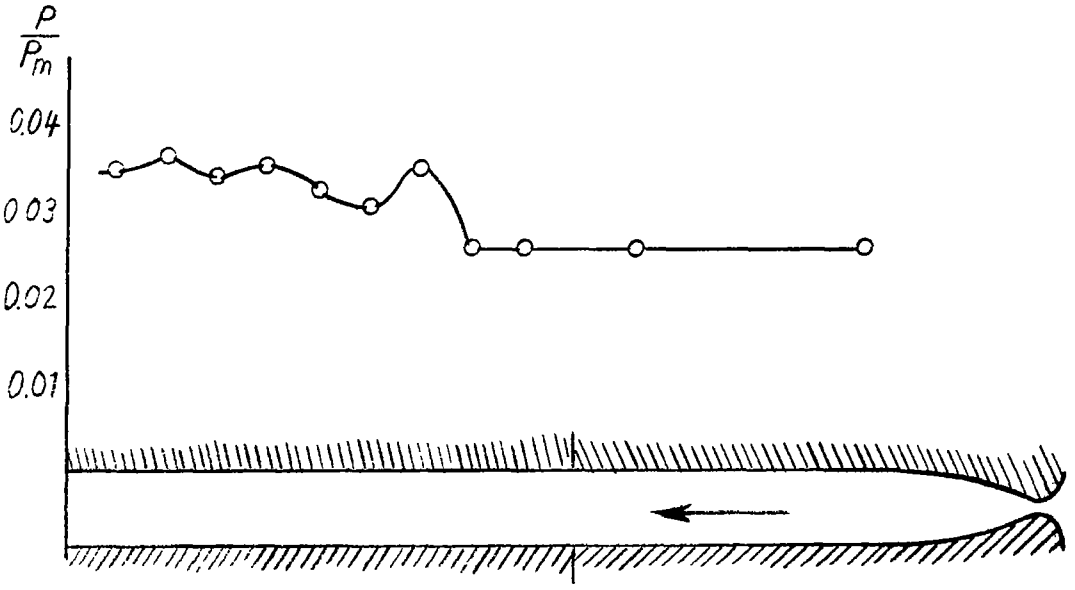

Figure 7a.- Pressure distribution in a parallel channel at supersonic speed.

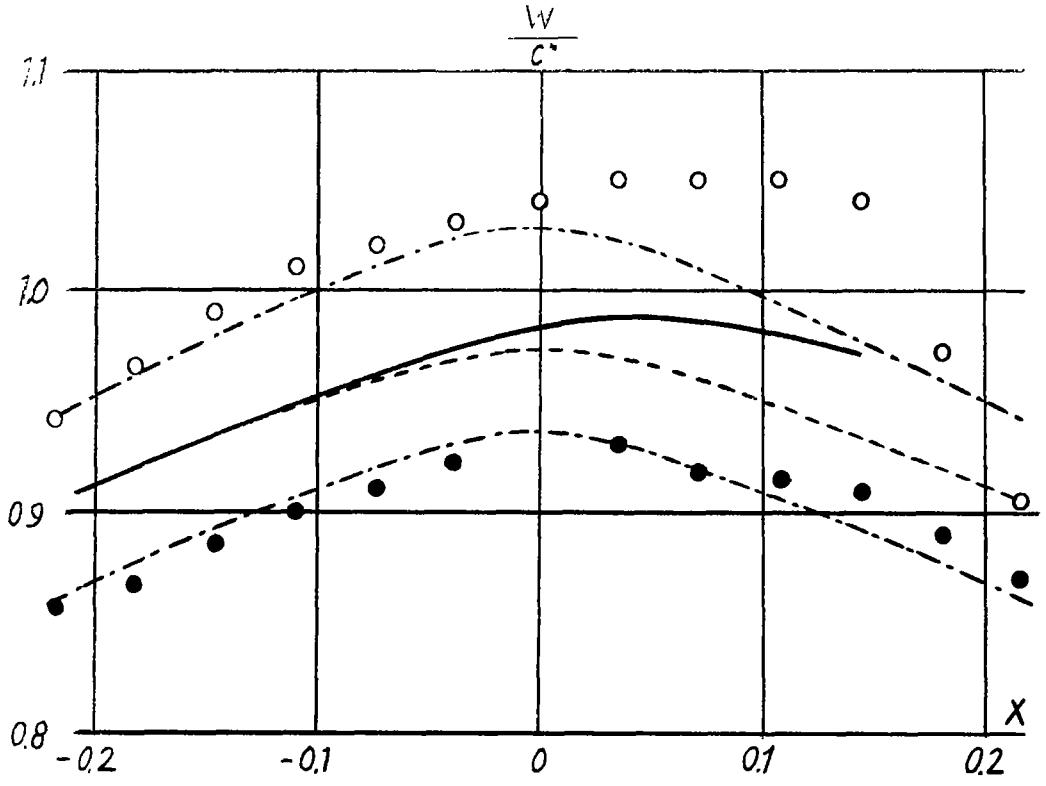

Figure 7b.- Velocity distribution in an axially summetrical nozzle according to Stanton (reference 1); test c.

● measured on the axis

o measured near wall

--- stream filament theory without boundary layer

—— stream filament theory with boundary layer

—·—· according to Oswatitsch and Rothstein (reference 2)

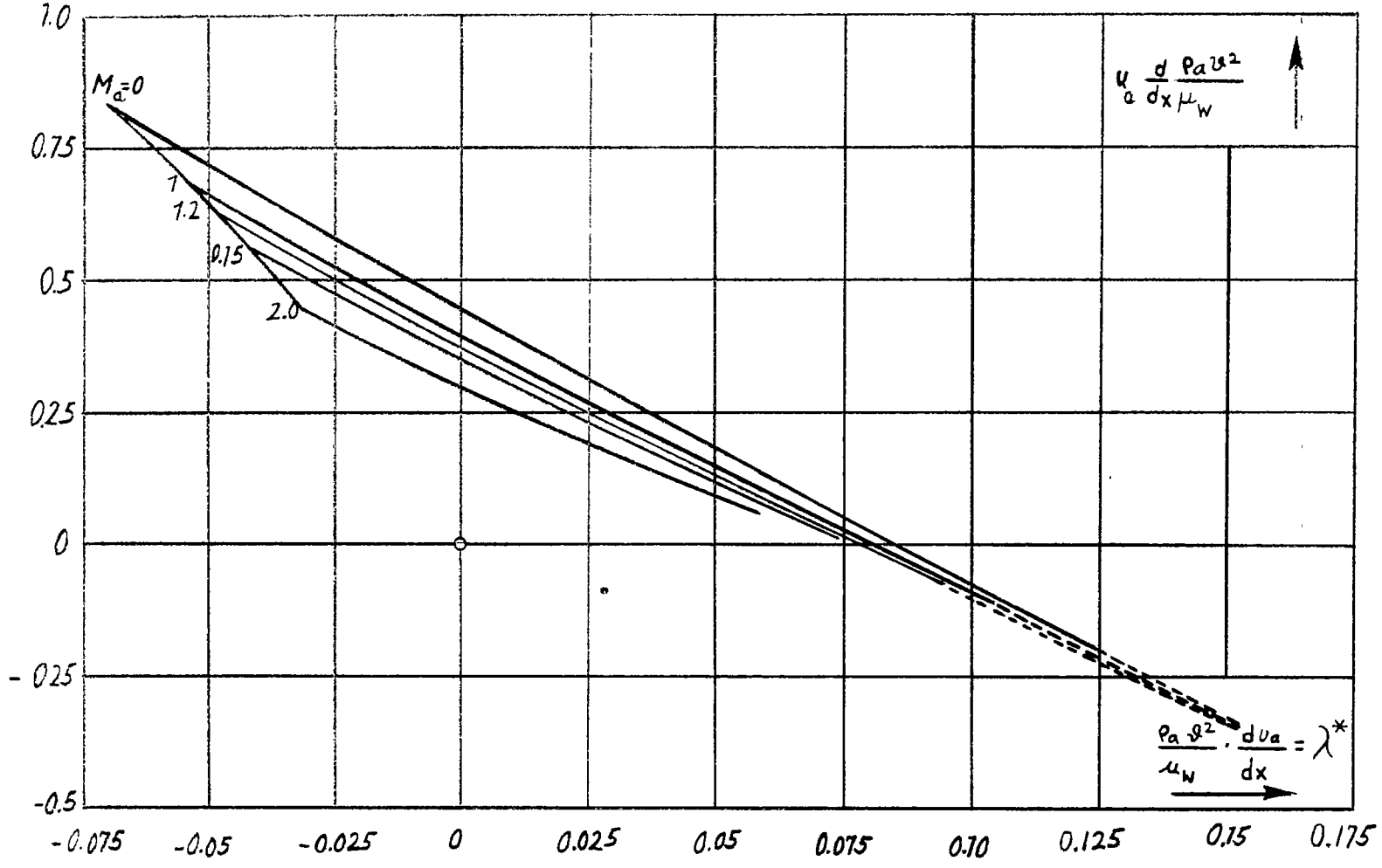

Figure 8.- Pohlhausen method for compressible boundary layers: $u_a \frac{d}{dx} \frac{\rho_a \vartheta^2}{\mu_w}$ plotted against λ^* for different Mach numbers.

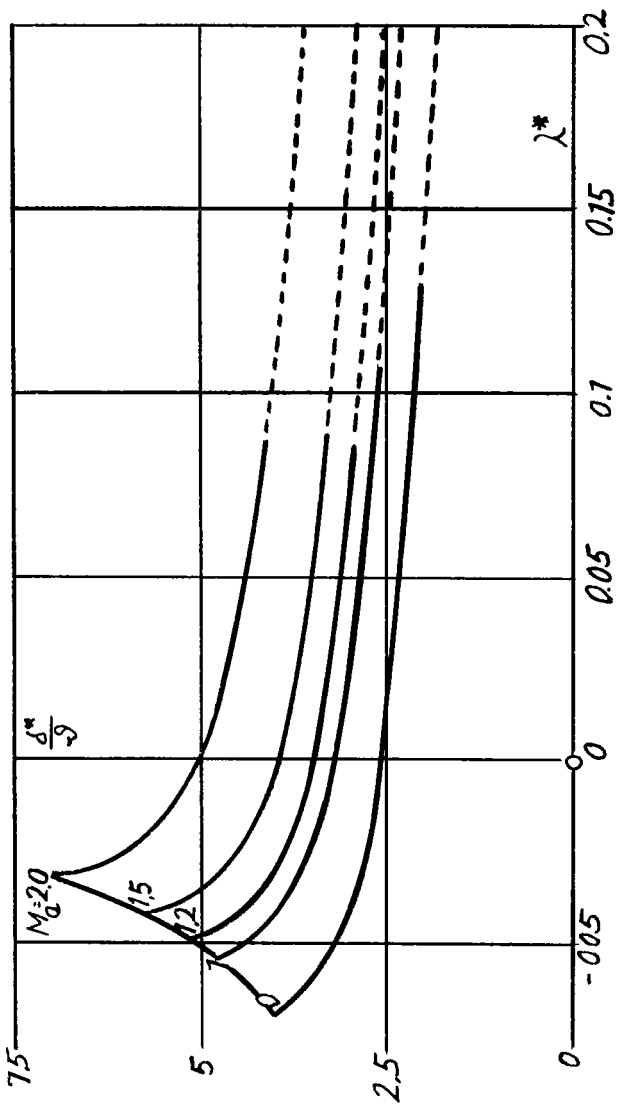

Figure 9.- Pohlhausen method for compressible boundary layers: δ^*/ϑ plotted against λ^* for different Mach numbers.

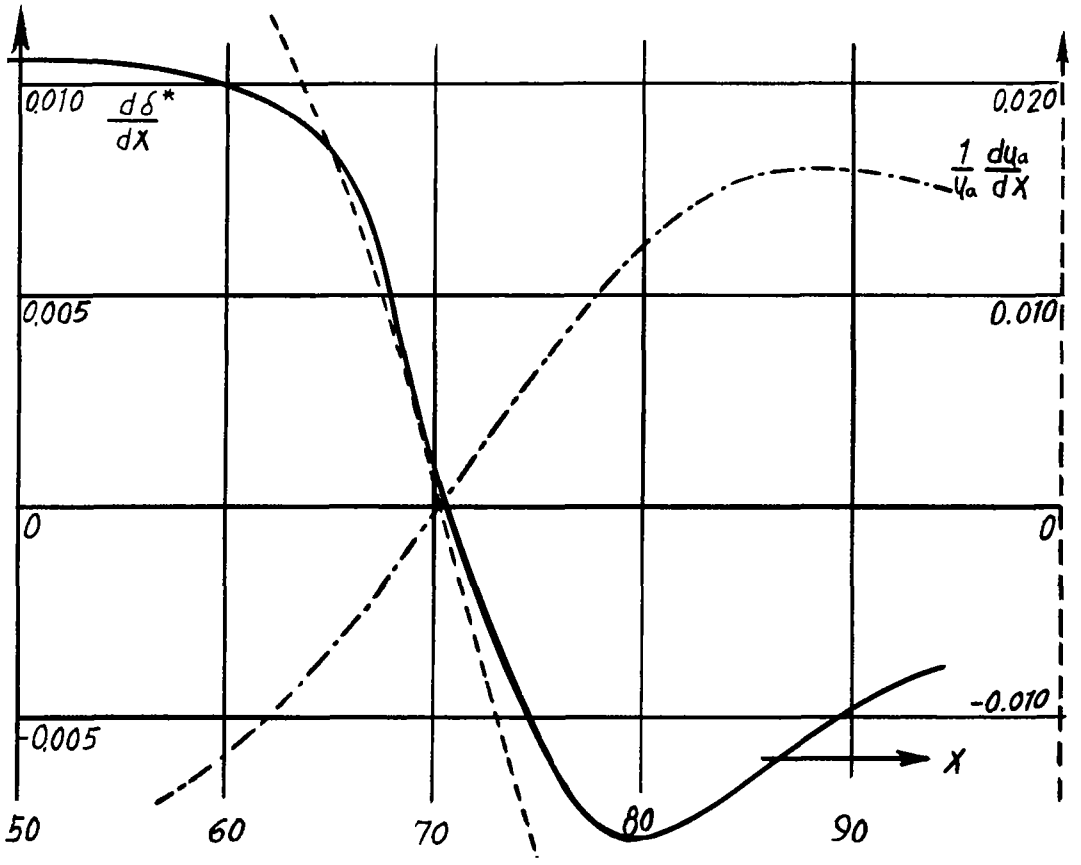

Figure 10.- Turbulent incompressible boundary layer. Gruschwitz test series 3 (reference 6):

—— $\frac{d\delta^*}{dx}$, — · — · — · $\frac{1}{u_a}\frac{du_a}{dx}$ on x

– – – – $\frac{d\delta^*}{dx}$ (from equation 5.9)

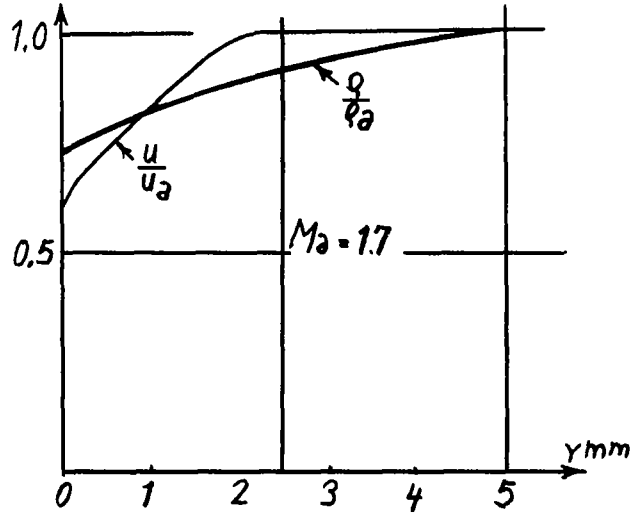

Figure 11.- Turbulent compressible boundary layer: velocity and density profile measured on the flat plate at Ma = 1.7.

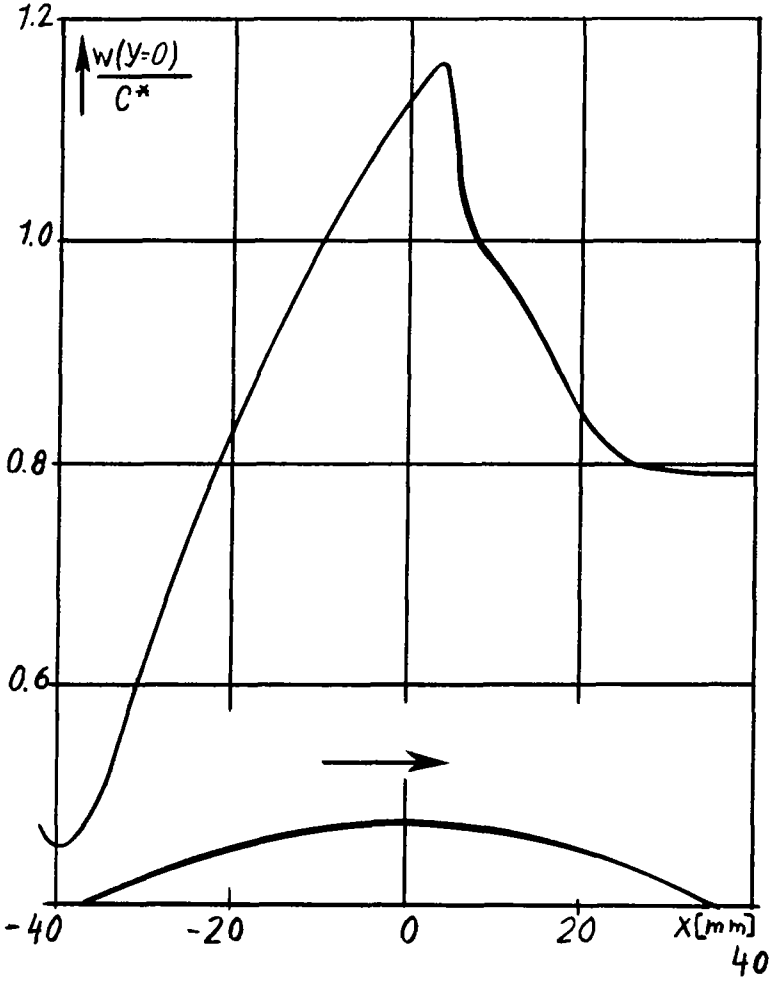

Figure 12.- Velocity distribution measured along a circular arc at a Ma number of flow of 0.61 (reference 12).

Page intentionally left blank

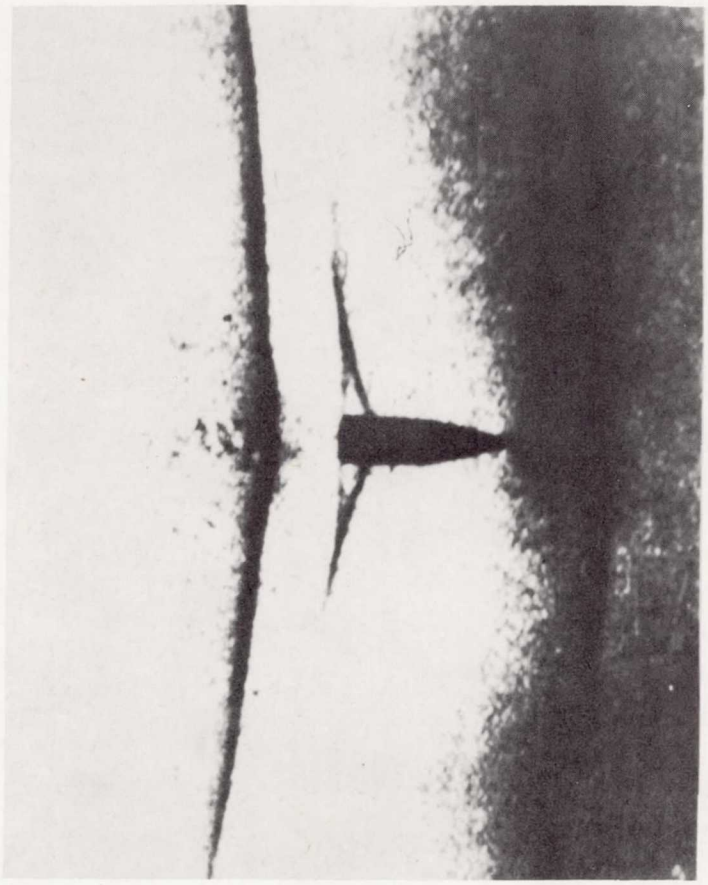

Figure 13.- Infantry bullet at slight supersonic speed (reference 9).